Barometers behaving badly II: A critical evaluation of Cpx-only and Cpx-Liq thermobarometry in variably-hydrous arc magmas

Penny E. Wieser[1,2], Adam J.R. Kent[2], Christy B. Till[3]

1. **Corresponding author**: Penny_wieser@berkeley.edu. Department of Earth and Planetary Sciences, McCone Hall, UC Berkeley, 94720, USA
2. College of Earth, Ocean and Atmospheric Sciences, Oregon State University, 97331, USA
3. School of Earth and Space Exploration, Arizona State University, Tempe, AZ 85281, USA

Key Words

- Clinopyroxene
- Thermobarometry
- Subduction Zones
- Arc magmatism
- Magma Storage Conditions

ABSTRACT

The chemistry of erupted clinopyroxene crystals (±equilibrium liquids) have been widely used to deduce the pressures and temperatures of magma storage in volcanic arcs. However, the large number of different equations parametrizing the relationship between mineral and melt compositions and intensive variables such as pressure and temperature yield vastly different results, with implications for our interpretation of magma storage conditions. We use a new test dataset comprised of the average Cpx-Liq composition from N=543 variably-hydrous experiments at crustal conditions (1 bar to 17 kbar) to assess the performance of different thermobarometers, and identify the most accurate and precise expressions for application to subduction zone magmas. First, we assess different equilibrium tests, finding that comparing the measured and predicted EnFs and K_D (using Fe_t in both phases) are the most useful tests in arc magmas, while CaTs, CaTi and Jd tests have limited utility. We then apply further quality filters based on cation sums (3.95-4.05), number of analyses (N>5), and the presence of reported H_2O data in the quenched experimental glass (hereafter 'liquid') to obtain a filtered dataset (N=214). We use this filtered dataset to compare calculated versus experimental pressures and temperatures for different combinations of thermobarometers. A number of Cpx-Liq thermometers perform very well when liquid H_2O contents are known, although the Cpx composition contributes relatively little to the calculated temperature. Most Cpx-only thermometers perform very badly, greatly overestimating temperatures for hydrous experiments. These two observations indicate that the Cpx chemistry alone holds very little temperature information in hydrous systems.

Cpx-Liq and Cpx-only barometers show similar performance to one another, with most expressions yielding RMSEs of 2-3.5 kbar. We also assess the sensitivity of different equations to melt H_2O contents, which are poorly constrained in many natural systems. Overall, this work demonstrates Cpx-based barometry on individual Cpx only provides sufficient resolution to distinguish broad storage regions (e.g., upper, mid, lower crust).

However, after significant amounts of averaging of Cpx compositions from experiments reported at similar pressures, RMSEs can reduce to ~1.3-1.9 kbar for the best-behaving expressions. We hope our findings motivate the substantial amount of experimental and analytical work that is required to obtain precise and accurate estimates of magma storage depths from Cpx±Liq equilibrium in volcanic arcs.

1. INTRODUCTION

The composition of erupted clinopyroxene (Cpx) and Cpx-liquid (Liq) pairs are commonly used to calculate pressures (P) and temperatures (T) in a variety of igneous systems. Cpx is a stable phase over a very wide range of pressures, temperatures, melt compositions and oxygen fugacities (e.g. Brugman and Till, 2019; Costa, 2004; Nandedkar et al., 2014; Ulmer et al., 2018), meaning Cpx-based thermobarometry has broad utility and has been applied in a wide variety of tectonic settings. Cpx is also a very common mineral in mafic to evolved magmas from volcanic arcs; as a result, Cpx-based barometry and thermometry has been widely applied in hydrous arc systems. However, recent work has also shown that there are limitations in our current state of knowledge about Cpx-based barometry and thermometry (Wieser et al., 2022a). Specifically, insufficient count times and/or low beam currents used for analysis of elements with concentrations (<0.5 wt%) yield highly imprecise measurements (1σ errors of 10–40% for Na2O) and insufficient characterization of the true composition of experimental Cpx. This low analytical precision causes large errors (± 3 kbar) in Cpx barometry when tested using global experimental datasets (Wieser et al., 2023a).

In this contribution, we investigate the sources of uncertainty associated with applying Cpx-based thermobarometers to determine storage conditions in variably hydrous arc magmas (e.g., Auer et al., 2013; Belousov et al., 2021; Cassidy et al., 2015; Caulfield et al., 2012; Cigolini et al., 2018; Dahren et al., 2012; Deegan et al., 2016; Freundt and Kutterolf, 2019; Geiger et al., 2018; Hollyday et al., 2020; Jeffery et al., 2013; Lai et al., 2018; Lormand et al., 2021; Moussallam et al., 2021, 2019; Namur et al., 2020; Preece et al., 2014; Romero et al., 2022; Ruth and Costa, 2021; Sas et al., 2017; Scruggs and Putirka, 2018; Sheehan and Barclay, 2016).

Existing expressions relating P and/or T to Cpx(±Liq) compositions are generally calibrated on experimental products conducted at known conditions, using a wide variety of equations based on multilinear regressions (e.g. Putirka, 2008, Neave and Putirka, 2017), or most recently, machine-learning techniques using decision trees (e.g., Petrelli et al. 2020, Jorgenson et al. 2021). Although a number of different Cpx-Liq and Cpx-only parametrizations exist (Neave and Putirka, 2017; Nimis, 1999; Petrelli et al., 2020; Putirka, 1999, 2008a; Wang et al., 2021), it is not always clear which parameterization is best, and how much the choice of equation affects geological interpretations. This is particularly true in volcanic arcs, where there has been no detailed evaluation of which thermobarometers behave best in variably hydrous arc magma compositions that occur in these settings. This is in contrast to extensive work evaluating thermobarometers in more H_2O-poor tectonic settings (e.g., Iceland, Neave et al., 2019; Neave and Putirka, 2017), and alkaline volcanic systems (Masotta et al., 2016; Mollo et al., 2013). Additionally, many existing calibrations

are also not parameterized in terms of water contents, and the underlying calibration datasets use a significant number of experiments where H_2O contents in experimental glasses are either not measured or are not reported (Wieser et al., 2023a).

The lack of consensus as to which thermobarometers are best is demonstrated by the breadth of choices selected by studies performing Cpx±Liq thermobarometry in arc magmas after the publication of the seminal thermobarometry review of Putirka (2008, Table 1). As many barometers contain a term for temperature, in natural systems where neither pressure not temperature is known, studies tend to iteratively calculate pressures and temperature using a thermometer and a barometer. Iteration of two equations greatly increases the number of possible combinations to perform calculations ($N_{barometers}$ X $N_{thermometers}$).

Table 1– Compilation of Cpx-based thermobarometers used in studies of arc magmas. In many studies, we deduced the exact equations used through email correspondence with the authors (many papers simply stated Putirka, 2008 in the text).

Clinopyroxene-Liquid barometry	
P = Putirka (2008) eq31, T = Putirka (2008) eq33	**P = Neave & Putirka (2017), T = Putirka (2008) eq33**
• Mt Baker and Glacier Peak, Cascades - *Sas et al. (2017)* • Whangaeuhu Gorge, New Zealand - *Auer et al. (2013)*	• Ebeko Volcano, Kurile arc - *Belousov et al. (2021)* • Lassen Peak, Cascades - *Hollyday et al. (2020)* • Lassen Peak, Cascades - *Scruggs and Putirka, (2018)* • Taupo Volcanic Zone - *Lormand et al. (2021)* • Calbuco Volcano - *Namur et al. (2020)*
P = Putirka (2008) eq30, T = Putirka (2008) eq33	**P = Putirka (2003), T = Putirka (2003)**
• Agung and Batur, Indonesia - *Geiger et al. (2018)* • Ambae, Vanuatu - *Moussallam et al. (2019)* • Ambrym, Vanuatu - *Moussallam et al. (2021)* • Ambrym, Vanuatu - *Sheehan and Barclay (2016)* • Villarrica, Chile – *Romero et al. (2022)*	• Agung and Batur, Indonesia - *Geiger et al. (2018)* • Ambrym, Vanuatu - *Sheehan and Barclay (2016*) • Soufrière Hills, Monseratt - *Cassidy et al. (2015)* • Krakatau, Indonesia - *Dahren et al. (2012)* • Tofua Volcano, Tonga - *Caulfield et al. (2012)*
P = Putirka (2008) eq32c, T = …	
T = Putirka (1996) eqT2 (spreadsheet default): • Mayon Volcano, Phillipines - *Ruth and Costa (2021)* **Thermometer not stated in paper:** • Miravalles-Guayabo Caldera, Costa Rica - *Cigolini et al. (2018)* • Mt Baker and Glacier Peak, Cascades - *Sas et al. (2017)*	**T = Putirka (2008) eq33:** • Chiltepe, Nicaragua - *Freundt and Kutterolf (2019)* **T = Putirka (2003)** • Agung and Batur, Indonesia - *Geiger et al. (2018)* • Merapi, Indonesia - *Preece et al. (2014)* • Krakatau, Indonesia - *Dahren et al. (2012)*
Cpx-only Barometry	
P = Putirka (2003) eq32b, T = …	**P = Putirka (2008) eq32a, T=…**
Thermometer not stated in paper: • Agung and Batur, Indonesia - *Geiger et al. (2018*) • Merapi Volcano, Indonesia - *Deegan et al. (2016)* • Ambae, Vanuatu - *Moussallam et al. (2019)* • Merapi, Indonesia - *Preece et al. (2014)* **T = Putirka (2008) eq32d:** • Kelut Volcano, Indonesia - *Jeffery et al. (2013*) **T = Putirka (2008) eq33:** • Chiltepe Volcanic Complex, Nicaragua - *Freundt and Kutterolf, (2019)*	**Thermometer not stated in paper:** • Taupo Volcanic Zone - *Beier et al. (2017)* **T from P2003:** • Volcan Melimoyu, Andes. *Geoffroy et al. (2018)* **T from P2008 eq32d:** • Ambrym, Vanuatu - *Sheehan and Barclay (2016)* • Ambrym, Vanuatu - *Moussallam et al. (2021)* **T from P2008 eq33:** • Mariana trough back-arc basin - *Lai et al. (2018)* • Okinawa Trough - *Chen et al. (2021)*

T from P1996: • Etna, Italy - *Ubide and Kamber, (2018)*	

Iteration of P and T from Putirka et al., (2003, hereafter P2003) has remained a popular choice even in recent years, despite the fact that more up-to-date recalibrations of these equations were provided in Putirka, (2008, hereafter P2008). Eq32c from P2008 is another popular barometer and has been iterated with a wide variety of different thermometers (Table 1). Another common choice is the iteration of P2008 eq30 or eq31 for pressure with eq33 for temperature. Alternatively, P2008 eq33 (T) has been iterated with the Neave and Putirka (2017, hereafter NP17) barometer. This choice is particularly interesting given that Neave and Putirka (2017) caution that their barometer may not be applicable to the more hydrous and oxidising conditions found in volcanic arcs.

Cpx-only thermobarometery has also been used for arc systems, but has been less popular than Cpx-Liq. Most studies have used the two Cpx-only barometers from Putirka (2008, eq32a for H_2O-independent, 32b for H_2O-dependent) iterated with a wide variety of different temperature estimates (e.g. Cpx-only and Cpx-Liq thermometers, Table 1). Three new Cpx-only thermobarometers have recently been published (Jorgenson et al., 2022; Petrelli et al., 2020; Wang et al., 2021), which will likely increase the use of Cpx-only equilibrium in a wide variety of tectonic settings, including volcanic arcs. Thus, it is important to evaluate their performance.

1.1 Comparison of existing thermobarometers

The diversity of published equations being used in the literature for Cpx-based thermobarometry is concerning because these equations can give different results for individual Cpx and Cpx-Liq pairs. To demonstrate the magnitude of these differences, we calculate pressures for 10 experiments from Blatter et al. (2017) performed at 7 kbar and 4 experiments from Blatter et al. (2013) performed at 4 kbar using the different combinations of equations highlighted in Table 1, and the most recently published thermobarometers (see also Supporting Fig. 1). We show error bars with the published RMSE for each barometer centered around the mean calculated P and T.

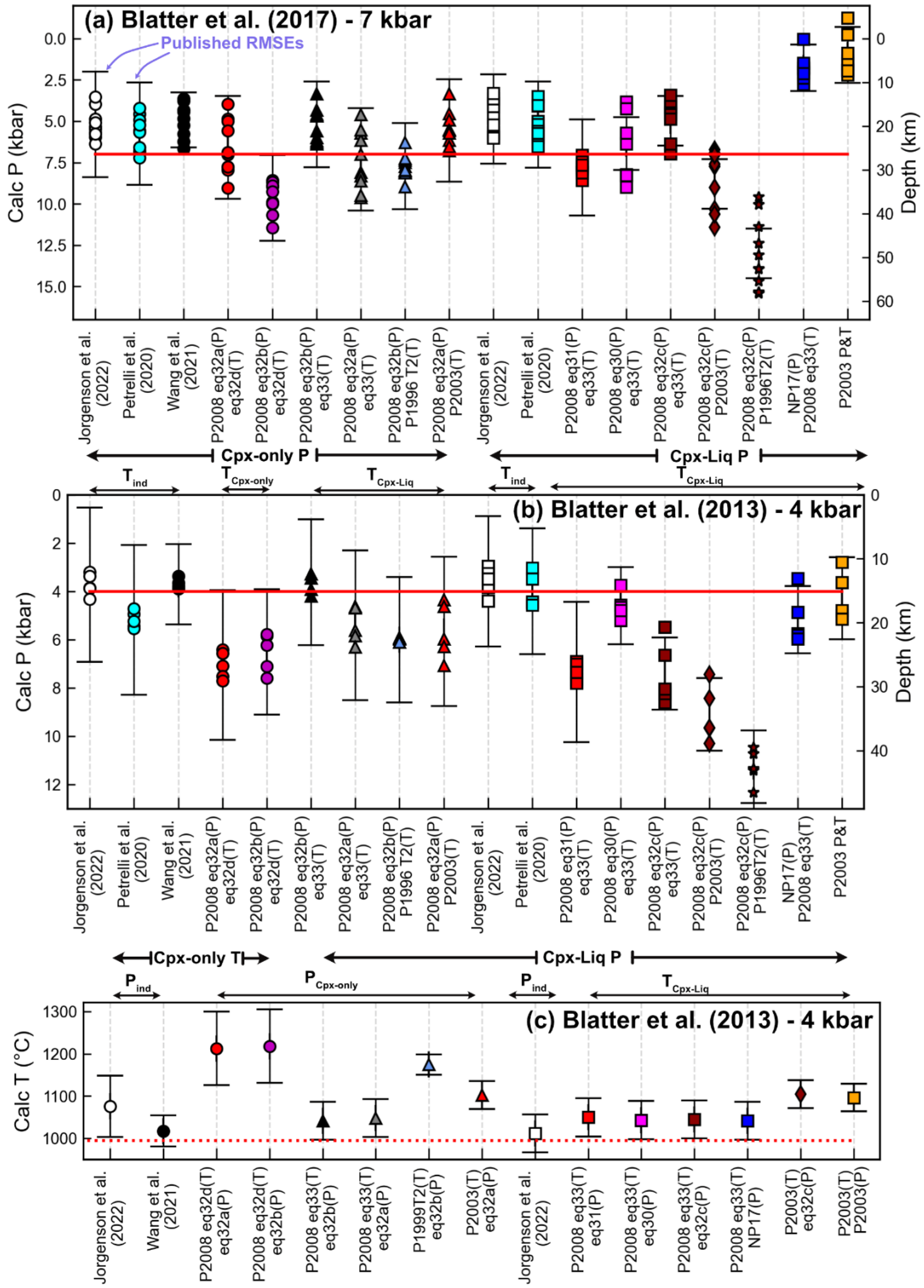

Figure 1 – Comparison of calculated P and T using the various combinations of thermometers and barometers summarized in Table 1. a) Pressure calculations performed for the 10 experiments of Blatter et al. (2017) performed at 7 kbar. b) Pressure calculations for the 4 experiments of Blatter et al. (2013) performed at 4 kbar. b) Temperatures calculated for experiment #2358 conducted at 995˚C, 5.5 wt% H2O, 9 kbar from Blatter et al. (2013). Error bars are plotted at the average

calculated P, and calculated T, showing the quoted RMSE from each equation. See Supporting Fig. 1 for an additional comparison.

Iteration of Neave and Putirka (2017) and P2008 eq33 (blue squares, Fig. 1a), or iteration of the PT expressions from Putirka (2003), would suggest storage at ~0-10 km, while iteration of P2008 eq32c with Putirka (1996) eqT2 (burgundy stars, Fig. 1a), would indicate storage at ~35-60 km depth. There is also no overlap between calculated pressures using the Cpx-only barometer of Jorgenson et al. (2022, white circles) and P2008 eq32b-32d (purple circles). Discrepancies also exist for the experiments conducted at 4 kbar from Blatter et al. (2013, Fig. 1b). The Cpx-Liq thermobarometers of Petrelli et al. (2020) and Jorgenson et al. (2022) suggest crystallization at ~15-20 km (mid crust), while iteration of P2008 eq32c for pressure with P2003 for temperature yields pressures in the lower crust (~35 km, brown diamonds), and the default iteration of eq32c in the P2008 spreadsheet indicates storage at >40 km depth (brown stars, Fig. 1a). Calculated Cpx-only temperatures show a very wide range (~200˚C) depending on the selected equation, while most Cpx-Liq temperatures lie within ~50-100˚C (Fig. 1c).

Despite these large discrepancies in calculated P and T using different equations, and obvious implications for geological interpretation, only a small proportion of studies applying Cpx-based barometers to natural systems have performed calculations using more than one thermobarometer (e.g., Erdmann et al., 2016, Erdmann et al., 2016; Geiger et al., 2018; Sas et al., 2017; Sheehan and Barclay, 2016). There is also a general lack of justification in the literature for why a specific equation was chosen. In many cases, the stated error statistics from the paper presenting the thermobarometers are quoted as the rational. For example, some studies appear to select their thermobarometers based on a smaller quoted SEE/RMSE from the original publication (e.g., Dahren et al., 2012; Preece et al., 2014). However, the way in which RMSE is calculated for these different equations is highly variable, so these statistics are not directly comparable. For example, Putirka et al. (2003) state a RMSE of ±1.7 kbar in their abstract based on the model fit to the calibration dataset (four studies, N=77 experiments). Similarly, Putirka (2008) states an RMSE of ±1.5 kbar for equation 32c based on the calibration dataset (four studies, N=99 experiments). These are the RMSEs quoted by Dahren et al., (2012) and Preece et al. (2014) to justify their use of these barometers. However, when Putirka (2008) applied these expressions to all available experimental data (n=1303), eq 32c has a SEE of ±5 kbar, and Putirka (2003) has a SEE of ±5 kbar for n=324 hydrous experiments, and ±4.8 kbar for 848 anhydrous experiments). Similarly, the SEE=±1.4 kbar commonly quoted by studies using the Neave and Putirka (2017) barometer reflects the fit to the calibration dataset (n=113), while the error on a global regression is ±3.6-3.8 kbar.

Assessing uncertainty using only the calibration data can greatly underestimate the true error (as the model has been tuned to those experiments). It is far more statistically robust to assess error using experiments that were not used during thermobarometer calibration (often termed a “test dataset”), especially when such test datasets share important compositional features

with target natural systems. Studies which state the more realistic errors associated with a test dataset in their abstract (e.g., Petrelli et al. 2020) may be less widely used simply because they have quoted a larger error, even though this error is more realistic.

Another issue associated with comparing published statistics and taking these as representative of the true error in natural systems is the variable pressure range of calibration and test datasets. For example, Petrelli et al. (2021) compute statistics for their test dataset using experiments conducted at 0-30 kbar, Putirka et al. (2003) from 0-35 kbar, and Neave and Putirka, (2017) from 0-20 kbar. However, it is uncommon that Cpx from the higher end of these pressure ranges are encountered when examining products from arc volcanoes. Using the compilation of crustal thicknesses from Profeta et al. (2016), all arc segments apart from the Northern and Central Volcanic Zone in Chile have Moho depths <45 km (~12 kbar), with these two thick-crusted settings Moho depths >50 km (~14-17 kbar). For the test dataset provided with the Cpx-only barometer of Petrelli et al. (2021), if experiments are restricted to those performed at 0-15 kbar, the R^2 value drops from 0.92 to 0.59.

Another factor that can affect the statistics presented for thermobarometers is that most thermometers have a pressure term, and most barometers have a temperature term. When assessing equation performance, most papers input the experimental temperature when calculating pressure, or the experimental pressure when calculating temperature. However, in natural systems, it is most common that neither pressure nor temperature is known, so a thermometer and a barometer must be selected, and iteratively solved (Table 1). This will increase the error compared to comparisons using experimentally-constrained pressures and temperatures (see Neave and Putirka, 2017).

Additional uncertainties when thermobarometers are applied to natural systems stem from the fact many equations have a term for the melt H_2O content. Iterative P-T calculations on experiments with known H_2O contents will underestimate the uncertainty associated with application to natural systems with uncertain H_2O contents. We investigate the sensitivity of different equations to H_2O to better constrain this often-neglected source of uncertainty.

To summarize - to get a realistic estimate of the errors associated with thermobarometry when applied to natural systems, we should be assessing performance using experimental datasets which were not used during calibration, iterating P&T, restricting comparisons to the pressure range of interest, and propagating uncertainty in melt H_2O content. Comparing calculated P and T from different equations for the samples of interest is also vital to assess systematic errors associated with the choice of thermobarometry equation(s). Unless one calibration can be robustly selected as the "best" for a given system, the range of P and T from different calibrations may be representative of the true uncertainty in calculated PT conditions. The best equation for a given system may be identified by compiling experiments with similar compositions to the system of interest and assessing which thermobarometry equations best reproduce the experimental values (e.g. Hammer et al., 2016; Neave and Putirka, 2017). Alternatively, if no suitable experimental data exists, insight may be gained by comparing the dataset used to calibrate each thermobarometry equation against the natural

compositions of interest to evaluate the degree of extrapolation required (e.g., Wieser et al., 2022b; Wieser et al., 2022c).

This discussion demonstrate that there is a clear need for igneous petrologists to be able to directly compare the suitability, accuracy and precision of different thermobarometric expressions when using thermobarometric calibrations in arc magmas (and other tectonic settings). In an effort to move towards this goal and evaluate the errors associated with calculations of magma storage conditions from Cpx in subduction zones, we compile a new experimental dataset of variably hydrous, tholeiitic to calc-alkaline compositions ranging from basalts to rhyolites. We ensure that none of the test dataset was used to calibrate each model we assess.

2. METHODS

2.1 ArcPL: a new test dataset for variably hydrous arc magmas

Our new test dataset is mostly comprised of experiments published since 2008, when the Library of Experimental Phase Relationship (LEPR) dataset used to calibrate most existing thermobarometers was formally compiled and made available to the community (Hirschmann et al., 2008). We also compile a handful of experiments which were conducted prior to 2008 but not included in the original LEPR compilation, (Berndt, 2004; Sisson et al., 2005). The full list of studies is as follows: Almeev et al., 2013; Andújar et al., 2015; Berndt, 2004; Blatter et al., 2023, 2017, 2013; Bogaerts et al., 2006; Cadoux et al., 2014; Costa, 2004; Erdmann and Koepke, 2016; Erdmann et al., 2016; Feig et al., 2010; Firth et al., 2019; Hamada and Fujii, 2008; Husen et al., 2016; Koepke et al., 2018; Krawczynski et al., 2012; Mandler et al., 2014; Marxer et al., 2022; Melekhova et al., 2015; Nakatani et al., 2022; Nandedkar et al., 2014; Neave et al., 2019, 2019; Parat et al., 2014; Parman et al., 2011; Pichavant and Macdonald, 2007; Rader and Larsen, 2013; Riker et al., 2015; Rutherford et al., 1985; Sisson et al., 2005; Solaro et al., 2019; Ulmer et al., 2018; Waters et al., 2021.

The liquid compositions in these studies have been normalized in different ways. In particular, many studies analysing glasses with high H_2O contents have reported oxides renormalized to 100% on an anhydrous basis, while others have reported analysed totals. For consistency, we normalize all glass analyses to have an anhydrous total of 100%.

For other parts of the discussion (e.g., assessing values of equilibrium tests), we also consider experiments conducted on compositions relevant to arc magmas that compiled in LEPR (Baker and Eggler, 1987; Barclay, 2004; Bartels et al., 1991; Berndt et al., 2001; Blatter and Carmichael, 2001; Di Carlo, 2006; Draper and Johnston, 1992, 1992; Feig et al., 2006; Gaetani and Grove, 1998; Grove et al., 2003, 1997, 1982; Hesse and Grove, 2003; Kawamoto, 1996; Martel et al., 1999; Mercer and Johnston, 2008; Moore and Carmichael, 1998). We refer to these experiments as ArcLEPR, and our newly compiled dataset as ArcPL (post-LEPR).

Our ArcPL dataset contains 543 Cpx-Liq pairs. There is a small amount of overlap with the training datasets of the most recent models (Jorgenson et al., 2022; Wang et al., 2021). These overlapping experiments are not used to test these specific equations. We restrict comparisons to experiments conducted at 0-17 kbar based on the crustal thickness

compilation of Profeta et al., (2016, assuming a crustal density of 2700 kg/m^3). The compositional, pressure (P) and temperature (T) range of this dataset is shown in Fig. 2. While 66% of Cpx-containing experiments in LEPR do not have compiled H_2O contents for experimental glasses, we endeavour to compile as much glass H_2O data as possible for our new dataset. In cases where glass H_2O data was not reported but the experiment was said to be volatile saturated we calculate dissolved H_2O using the solubility model MagmaSat (Ghiorso and Gualda, 2015; implemented in VESIcal; Iacovino et al., 2021) using the quoted experimental P, T and the fluid composition if given (X_{H_2O}). MagmaSat has been shown to provide the best fit to arc magma compositions (Wieser et al., 2022c). Overall, only 22% of our ArcPL dataset has missing H_2O data, and these experiments are not considered when assessing thermobarometers (see Section 2.2).

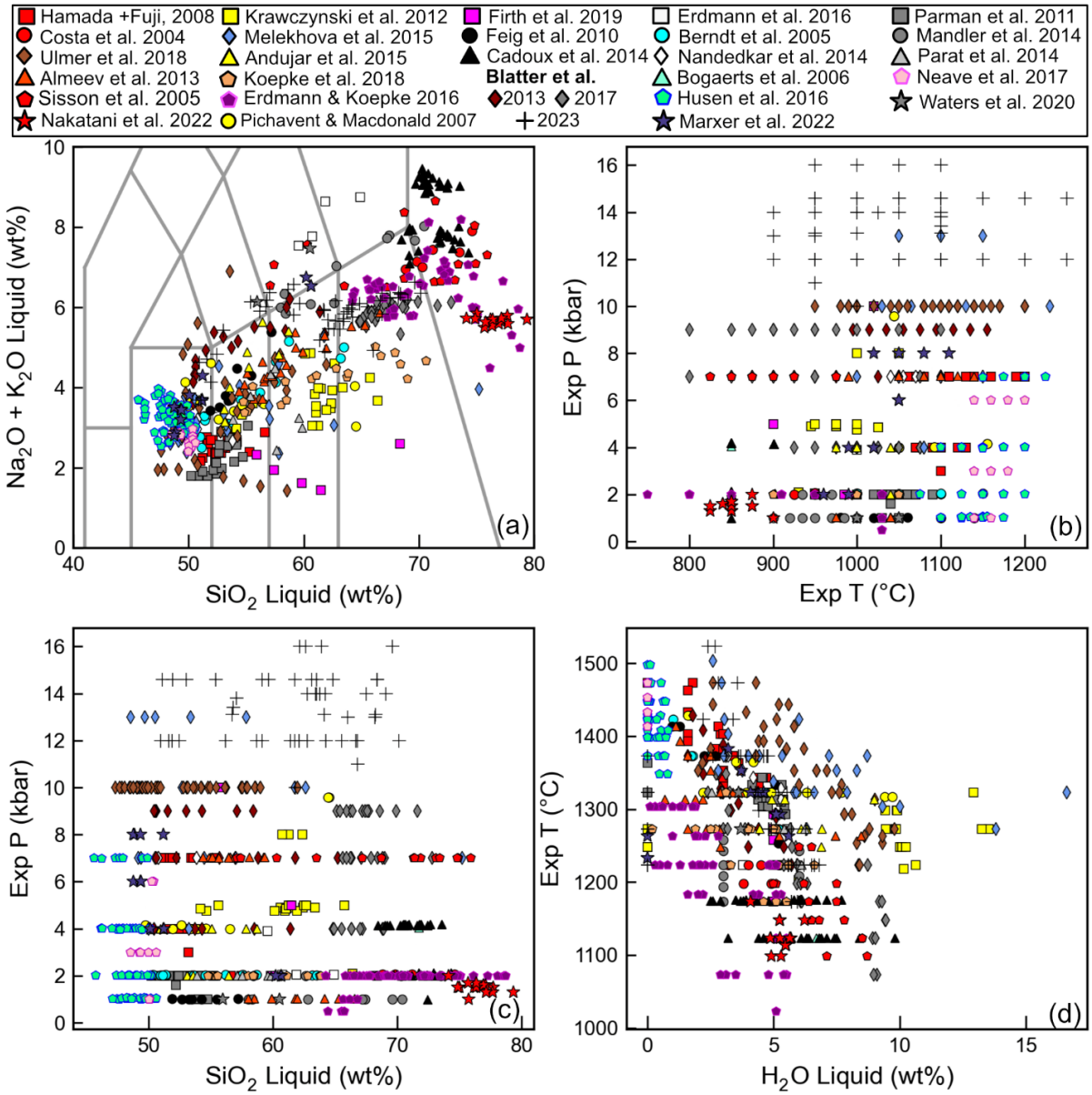

Figure 2 – Compositional and P-T spread for the ArcPL dataset before the application of filters for Cpx-Liq equilibrium, cation sums, number of analyses and melt H_2O contents.

2.2 Equilibrium Tests

One of the main issues when performing Cpx-Liq thermobarometry in natural systems is selecting which measured Cpx compositions to pair with which liquid compositions. In arc (and other tectonic settings), it is difficult to identify and sample erupted liquids that were in equilibrium with a given Cpx. A number of different literature studies have taken the approach of compiling all available whole-rock and glass data from the volcanic system and considering all possible matches between Cpx and these Liq compositions, discarding pairs which fall outside preferred ranges of several equilibrium tests (Gleeson et al., 2021; Neave et al., 2019; Scruggs and Putirka, 2018). This approach, although popular, is also strongly reliant on having reliable tests by which to assess Cpx-Liq equilibrium. Equilibrium filters have also been applied to experimental datasets when calibrating thermobarometers (Neave and Putirka, 2017). However, a variety of equilibrium tests and cut off values have been proposed, and it is not always clear what values should be used. Thus, we start by evaluating commonly used filters using the ArcPL dataset.

The most widely used equilibrium test assesses partitioning of Fe-Mg between clinopyroxene and liquid ($K_{D,\ Fe-Mg}^{Cpx-Liq}$ abbreviated as K_D). Putirka (2008) calibrate an expression (eq35) using LEPR experiments to calculate K_D solely as a function of temperature:

$$K_D = e^{-0.107 - \frac{1719}{T\,(K)}}$$

There is ambiguity in the thermobarometry literature as to the best way to compute the measured value of K_D from EPMA measurements of Fe-Mg in the Cpx and Liq. Some studies perform the calculation using only Fe^{2+} in the liquid and Fe_T in the Cpx (e.g., Neave et al. 2017, Gleeson et al. 2020), while others use the total amount of Fe (Fe_T) in the liquid (Putirka et al. 2016). It is important to work out which approach works better prior to discarding specific Cpx-Liq pairs, particularly in experiments and natural samples from arcs, which are generally quite rich in Fe^{3+} (Carmichael, 1991; Kelley and Cottrell, 2009).

We calculate the proportion of Fe^{2+} in each experiment using the experimental fO_2, with the equations of Kress and Carmichael (1988) implemented in Thermobar (an open-source Python-based thermobarometry tool, Wieser et al., 2022b, Fig. 3). If fO_2 is not given, we calculate it from the quoted buffer position, experimental pressure and temperature. For completeness of our assessments, we also calculate Fe^{2+} in the Cpx using the method of (Lindsley, 1983, acknowledging stoichiometric methods estimating Fe^{2+} in minerals are associated with large errors), and calculate K_D using just Fe^{2+} in both phases.

K_D values are significantly closer to predicted values from Putirka (2008) when Fe_T in both the liquid and Cpx are used (Fig. 3a). When using Fe^{2+} in the liquid and Fe_T in the Cpx (red dots, Fig. 3b), many more experiments lie outside the ±0.08 window around the predicted value for Putirka (2008), particularly for experiments with >30% Fe^{3+} (Fig. 3d). Using Fe^{2+} in the Liq and Cpx (black squares, Fig. 3b) also results in more experiments failing the equilibrium test. The superior performance using just Fe_T is perhaps unsurprising, given that eq35 of Putirka (2008) was calibrated using Fe_T. Thus, we suggest that until equilibrium tests

are recalibrated on a substantial volume of experimental data with well constrained Fe^{2+} proportions in liquid (and Cpx), it is best to use Fe_T in both phases for consistency with the calibration of eq35. Using Fe^{2+} in the liquid could lead to more oxidised experiments (or natural samples) being discarded incorrectly (Fig. 3d). It is also interesting that the ±0.03 filter used by many authors (Neave et al., 2019, Scruggs and Putirka, 2018) would exclude a large amount of experimental data (66%), while the ±0.08 value from Putirka (2008) only results in 23% of data being discarded (±0.03 marked by dotted lines, ±0.08 by the grey box on Fig. 3). While deviation from the predicted equilibrium values may represent true disequilibrium in experiments, to retain a reasonably sized dataset, we proceed with the following comparisons using only experiments with measured K_D values that are within ±0.08 of predicted values calculated from eq35 of Putirka (2008).

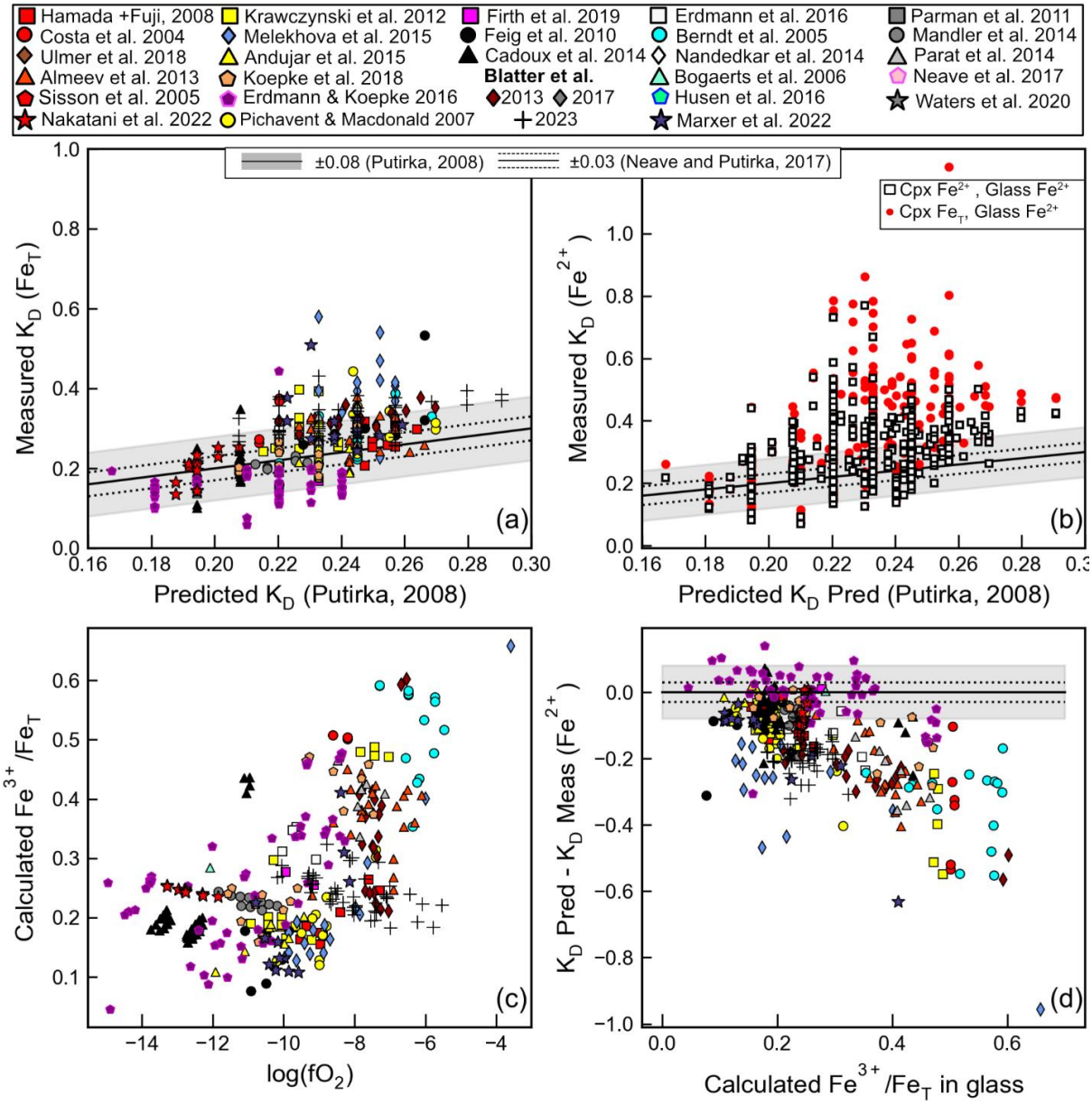

Figure 3 - Assessment of Fe-Mg partitioning between Cpx and Liq (K_D) in the ArcPL dataset. a-b) Predicted values calculated using Putirka (2008) eq35. vs. measured values. In a), Fe_T is used in Cpx and Glass to calculate the measured value. In b) the red dots show calculations using Fe^{2+} in the liquid calculated using Kress and Carmichael (1988) from the quoted experimental fo_2 or redox buffer (see

part c), and Fe_T in the Cpx. Black squares show Fe^{2+} in the liquid and Fe^{2+} in the Cpx calculated using Lindsley and Andersen (1983). d) The discrepancy between calculated and predicted K_D values using Fe^{2+} in the liquid and Fe_T in the Cpx increases with increasing proportion of $Fe^{3.}$ Dashed lines show the ±0.03 value used for equilibrium tests by Neave et al. (2019), while the grey field shows the ±0.08 value suggested by Putirka (2008).

Wood and Blundy, (1997) also propose an expression:

$$K_D = 0.109 + \frac{0.186}{Mg\#\ Cpx}$$

We find that this performs very poorly, with the offset between calculated and predicted K_D correlating with Cpx Mg# (Supporting Fig. 2).

Comparing the predicted and measured value of the Ca-Tschermak's (CaTs) component is another popular equilibrium test, with most studies using the expression of Putirka (1999) to calculate the predicted CaTs value (e.g., Gleeson et al., 2021; Neave et al., 2019). In the ArcPL dataset, there is a very poor correspondence between predicted and measured CaTs values (Fig. 4a). This is also true for experiments from LEPR conducted on compositions relevant to arc magmas (ArcLEPR, red crosses, Fig. 4a). The discrepancy between predicted and measured values is most apparent at higher measured values of CaTs (Fig. 4a), and correlates most strongly with the Al^{VI} content of the Cpx (Fig. 4b). Al^{VI} in Cpx is one of the key parameters used to calculate the CaTs component:

$$CaTs = Al^{VI} - X_{Na}$$

This means that it is not possible to resolve this offset simply by adding in a term for Al^{VI} in the expression for predicting this component from the liquid component (as this would make it a useless equilibrium test). Clearly, the terms for liquid components, pressure and temperature used in the Putirka (1999) expression to predict the CaTs component are insufficient to account for variation in CaTs in experimental Cpx in hydrous experiments. While the RMSE=±0.07 value of Putirka (1999) would result in most experimental pairs being "in equilibrium", use of the ±0.03 filter of Neave et al. (2019) would cause a significant number of experimental pairs to be discarded. Given the poor correlation between predicted and measured values, and the correlation of the discrepancy with $Al^{VI,}$ we suggest that CaTs in its current state is not a useful equilibrium test when working with arc magmas.

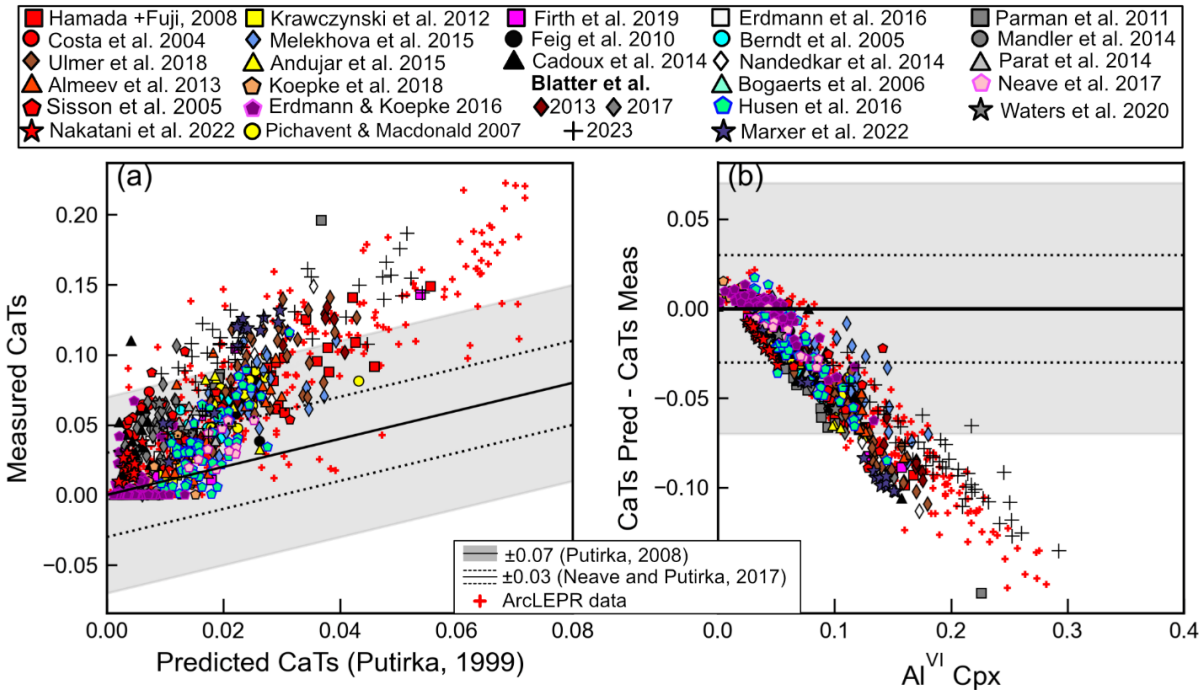

Figure 4 – a) Comparison of predicted and measured values of CaTs. The grey colored box shows the ±0.07 error window suggested by Putirka (1999), and the dashed lines show the ±0.03 value used by Neave et al. (2019) to filter natural Cpx-Liq pairs. b) There is a strong correlation between the discrepancy and the Al^{VI} component of Cpx.

The measured Enstatite-Ferrosillite (EnFs) component shows good agreement with the predicted components using the equation of Mollo et al. (2013) for ArcPL (Fig. 5b) and ArcLEPR (Fig. 5a). Relatively few values lie outside the ±0.05 error window. In contrast, measured Diopside-Hedenbergite (DiHd) values show poor agreement with predicted values using Mollo et al. (2013) for lower temperature experiments, particularly in the ArcPL dataset (Fig. 5c-d). The discrepancy is even worse if DiHd is predicted using Putirka (1999). The overprediction of calculated DiHd values at low temperatures appears to result from the high T-sensitivity of the Mollo et al. (2013) expression at these temperatures. To demonstrate this, we calculate predicted DiHd values for temperatures of 750-1400°C using 20 randomly-selected Cpx-Liq pairs. Below ~1000°C, the predicted value rapidly kicks up to higher values (Fig. 5e, red lines). When the measured values for these 20 pairs are subtracted from the predicted value, the resulting curves recreate the trend to higher values seen in the whole dataset, indicating that this strong temperature-dependency is the cause of the discrepancy (Fig. 5f). The expressions of Mollo et al (2013) were calibrated using LEPR which contains relatively few experiments at these low temperatures (white squares, Fig. 5f). The lower temperatures of our dataset relative to their calibration range likely result from the higher H_2O contents. These results suggest that care should be taken when applying a DiHd filter to clinopyroxene-liquid pairs in arcs that may have crystallized below 900-1000°C, and that this expression likely needs recalibrating with a dataset of lower temperature experiments.

Finally, lesser used equilibrium tests are also of questionable utility. Only two Cpx-Liq pairs in ArcPL have a measured CaTi component outside the 1σ range of Putirka (1999, Fig. 6a), but there is a poor correlation between predicted and measured values (indicating it is not a useful test). There is a similarly poor correspondence between predicted and calculated Jd components, with the discrepancy correlating as a function of the Na_2O content of the Cpx (the main component used to calculate Jd, Fig. 6b-c). As for CaTs, this means that recalibration without knowing the Cpx composition is unlikely to be successful.

Overall, these comparisons demonstrate that EnFs, DiHd (for Cpx crystallized at >1000˚C), and K_D calculated using Fe_T with a filter of ±0.08 rather than ±0.03 are currently the most robust tests of equilibrium when assessing possible Cpx-Liq pairs in arc magmas. Because of the wide range of temperatures in our compiled dataset, we filter our ArcPL dataset to include only experiments within =±0.08 of the predicted value for K_D (using Fe_T) and within ±0.05 for EnFs. We also only include clinopyroxenes with [Ca/(Ca+Mg+Fe) atomic] between 0.2 and 0.5 (i.e. excluding pigeonites), and cation sums between 3.95 and 4.05. To help alleviate random scatter associated with analytical imprecision, we only use experiments that measured at least 5 Cpx in each experimental charge (see Wieser et al., 2022a). As many of the thermobarometers assessed here contain a term for H_2O, we also only consider experiments with some form of reported H_2O contents (e.g., SIMS, FTIR or Raman measurements, volatiles-by-difference, or enough information to calculate H_2O using a solubility model). Of the compiled N=543 new experimental charges, N=123 fail the K_D filter, N=71 fail the EnFs filter, N=20 fail the cation sums filter, N=156 fail based on having <5 Cpx analyses, and N=53 are discarded based on having no reported H_2O data (see Supporting Fig. 3). Obviously, some experiments fail multiple criteria. Overall, we are left with N=214 experimental charges. We use these experiments to assess the best performing thermobarometers in arc magmas.

Figure 5 - Comparison of measured values of EnFs and DiHd with those predicted from the expression of Mollo et al. (2013). In a), the grey bar shows ±0.05, while in b), the grey bar shows ±0.06 (both cut offs from Mollo et al. 2013). Symbols are coloured based on the experimental temperature. e) Predicted values of DiHd as a function of temperature using the expression of Mollo et al. (2013) for 20 randomly-selected Cpx-Liq pairs. e) The discrepancy between predicted and measured DiHd contents for these 20 Cpx (red lines), with experimental data from Arc-PL (black dots) and LEPR (white squares) overlain.

Figure 5 - Comparison of measured values of EnFs and DiHd with those predicted from the expression of Mollo et al. (2013). In a), the grey bar shows ±0.05, while in b), the grey bar shows ±0.06 (both cut offs from Mollo et al. 2013). Symbols are coloured based on the experimental temperature. e) Predicted values of DiHd as a function of temperature using the expression of Mollo et al. (2013) for 20 randomly-selected Cpx-Liq pairs. e) The discrepancy between predicted and measured DiHd contents for these 20 Cpx (red lines), with experimental data from Arc-PL (black dots) and LEPR (white squares) overlain.

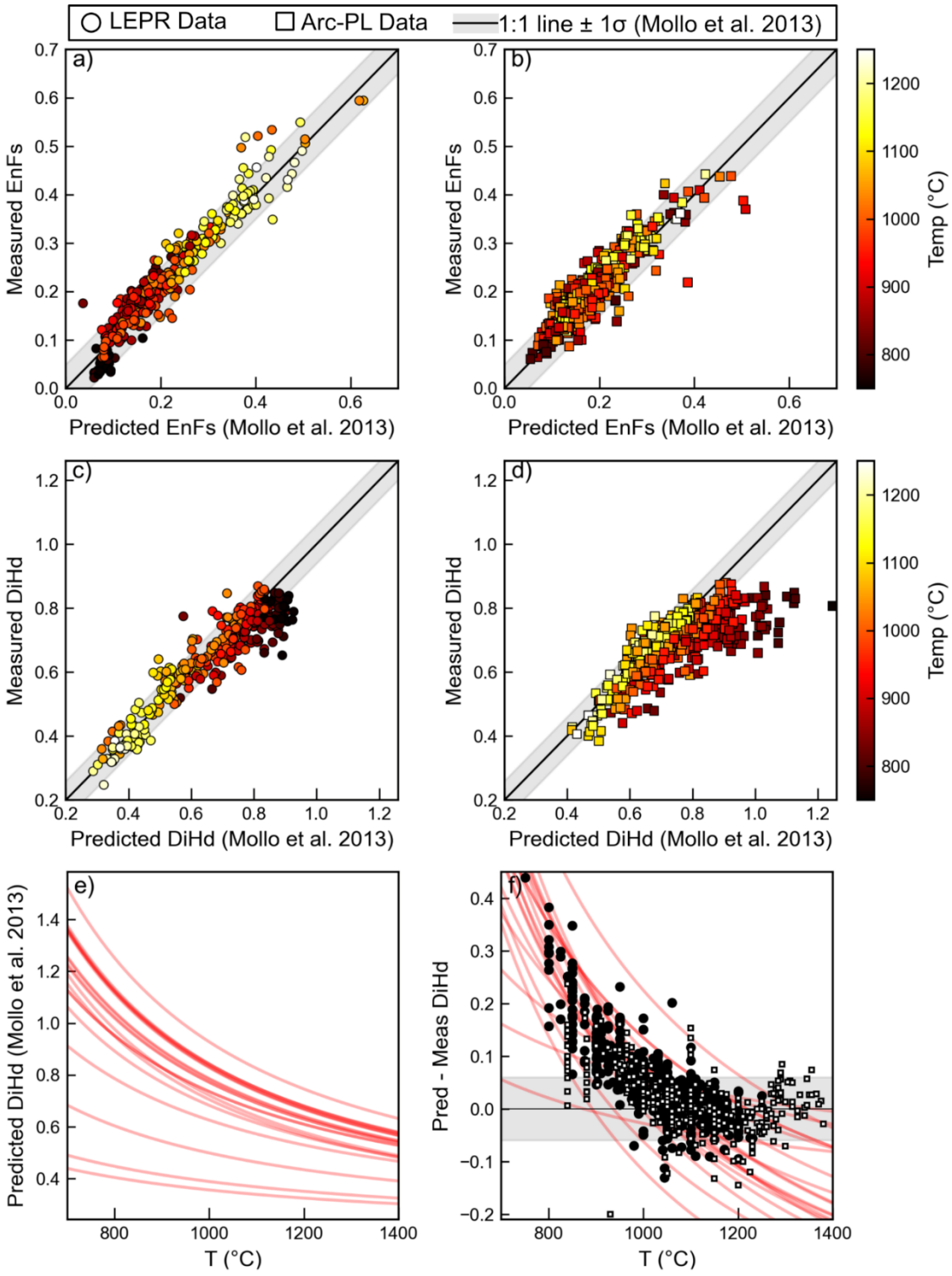

Figure 5 - Comparison of measured values of EnFs and DiHd with those predicted from the expression of Mollo et al. (2013). In a), the grey bar shows ±0.05, while in b), the grey bar shows ±0.06 (both cut offs from Mollo et al. 2013). Symbols are coloured based on the experimental temperature. e) Predicted values of DiHd as a function of temperature using the expression of Mollo et al. (2013) for 20 randomly-selected Cpx-Liq pairs. e) The discrepancy between predicted and measured DiHd contents for these 20 Cpx (red lines), with experimental data from Arc-PL (black dots) and LEPR (white squares) overlain.

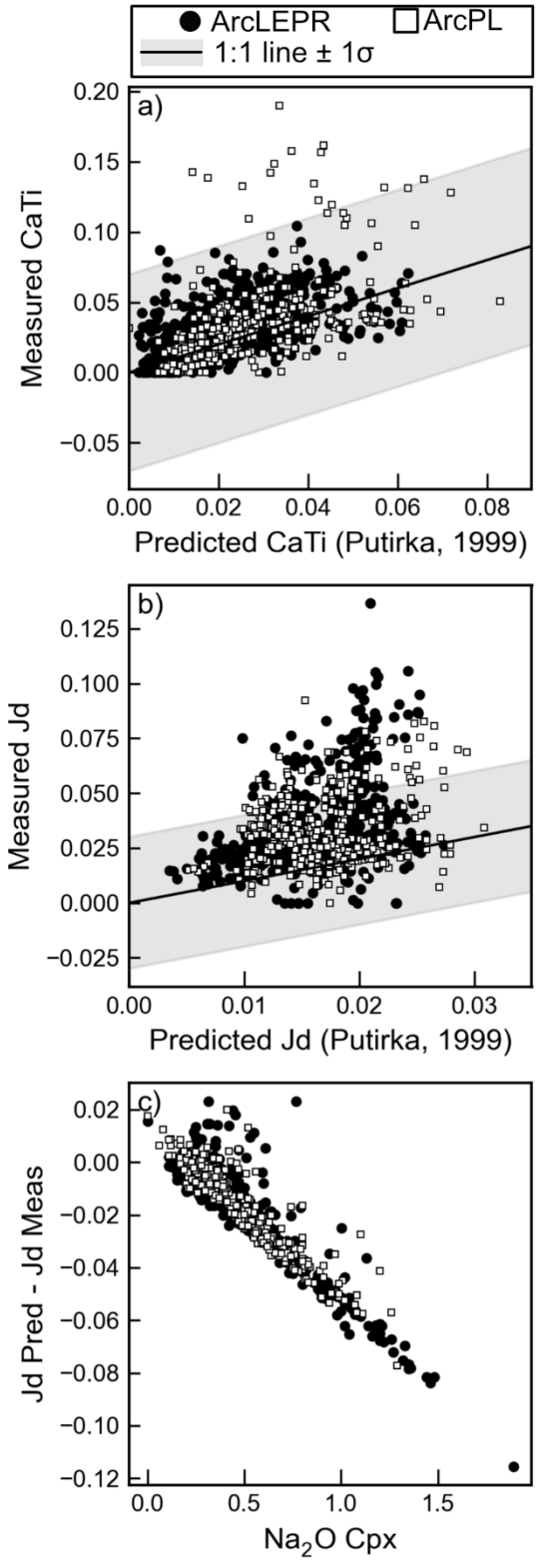

Figure 6 - The discrepancy between calculated and measured a) CaTi and b) Jd components. The discrepancy increases as a function of Na_2O content of the Cpx.

2.3 Statistical metrics used in this paper

To assess thermobarometer performance, we calculate the statistics for a linear regression between experimental P or T (x) and calculated P and T (y), and use five statistical metrics associated with this regression to assess the performance of the equation: the correlation coefficient (R^2), the gradient and intercept of the regression, the root mean square error (RMSE) and the mean absolute error (MAE), where:

$$RMSE = \sqrt{\frac{1}{N}\sum_{i=1}^{N}(x_i - y_i)^2}$$

$$MAE = \frac{1}{N}\sum_{i=1}^{N}(x_i - y_i)$$

The MAE doesn't have a squared term like the RMSE, such that it can more easily identify systematic uncertainty. The gradient of the regression and the intercept also helps identify systematic uncertainty.

3. DISCUSSION

3.1. Assessing Cpx-Liq thermobarometers

When estimating temperature from Cpx-Liq equilibrium, iteration of the temperatures calculated using eq33 of P2008 with a variety of different barometers (P2008 eq30, P2008 eq32c, and NP17) do a good job of reproducing experimental temperatures in the ArcPL dataset (Fig. 7a-c). The best fit is obtained from iteration of P2008 eq33 with Neave and Putirka (2017, Fig. 7a), returning an R^2 value of 0.92, a gradient close to 1 (0.94), and an intercept of ~93°C. This iteration also has the lowest RMSE (31.8°C) and MAE (13.6°C).

Iteration of the thermometer and barometer of Putirka et al. (2003) substantially overestimates

464 temperature (Fig. 7d, MAE=79°C, RMSE=90.5°C), and the discrepancy is correlated with the
465 melt H_2O content (Supporting Fig. 4a). This is unsurprising given this equation does not
466 contain a term for H_2O in the liquid (Putirka, 2008). However, this offset is concerning as this
467 equation has been applied to hydrous arc magmas (Table 1).

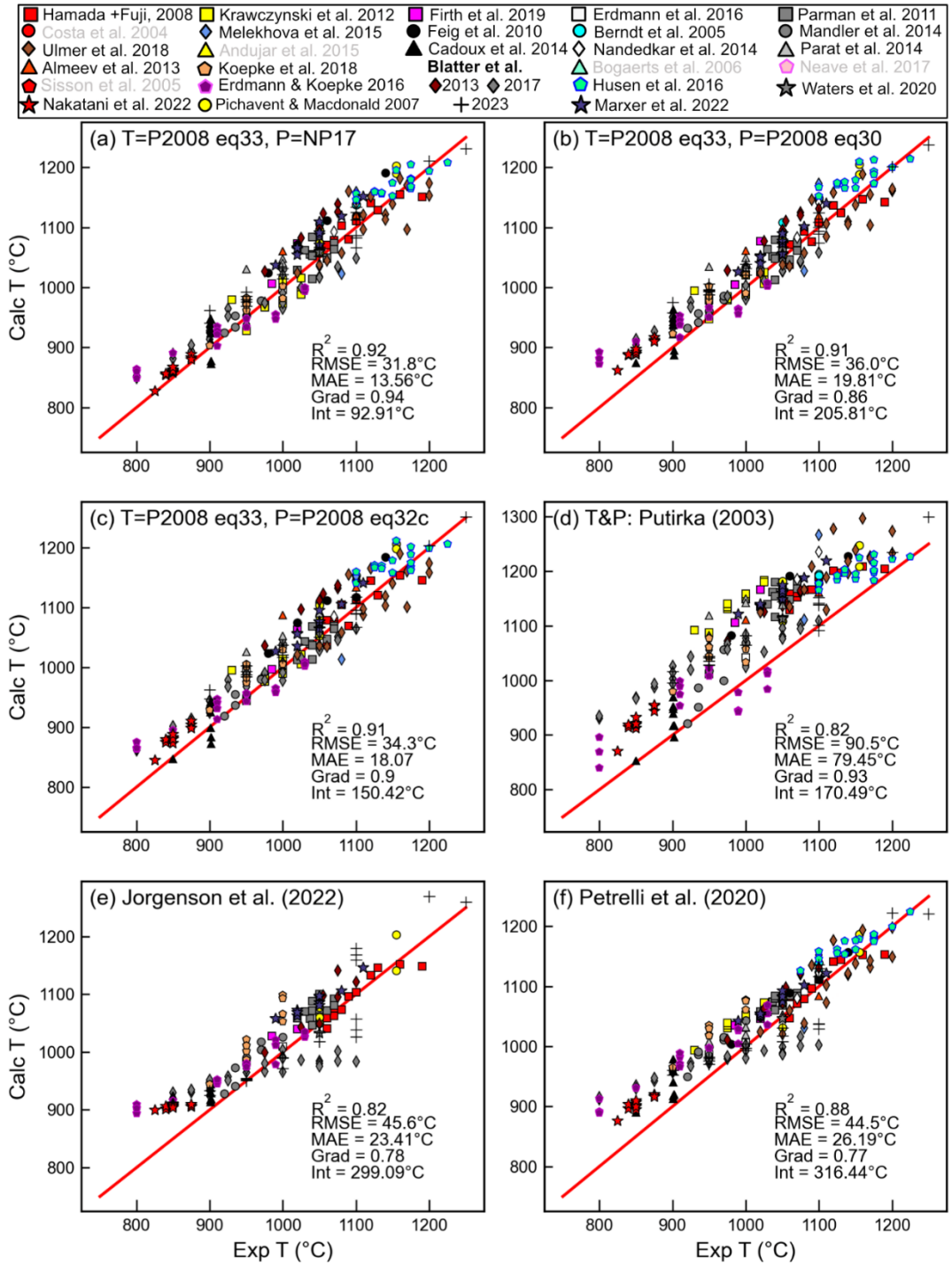

468

469 *Fig. 7 – Evaluation of various Cpx-Liq thermometers (iterating P and T) for the filtered ArcPL dataset.*
470 *Experimental studies shown in Fig. 2 where all charges failed equilibrium or quality filters are greyed*
471 *out in the legend. The best thermometer for this dataset is Putirka (2008) eq 33 iterated with Neave*
472 *and Putirka (2017), indicated by the gold trophy symbol. When testing the Jorgenson et al. (2022)*

expression, experiments in their calibration dataset are excluded, resulting in fewer symbols being shown on this panel than others. A red 1:1 line is shown on each plot.

The machine-learning P-independent thermometer of Petrelli et al. (2020) yields worse statistics than P2008 eq33 for the ArcPL test dataset, largely because of its poor performance at <1000°C, where it overpredicts temperature (Fig. 7f). Overprediction at low values, and underprediction at high values is common for regression tree methods, as these algorithms will not return a value outside the calibration range of the training dataset. As some of the experiments in ArcPL were used to calibrate the machine learning thermobarometer of Jorgenson et al. (2022), we exclude these data when assessing this equation (Fig. 7e). For the Jorgenson et al. (2022) thermobarometers, the authors recommend using the median value calculated across all trees, rather than the mean as used by Petrelli et al. (2020). For the ArcPL dataset, the median and mean show very similar results for temperature (Supporting Fig. 5c-d), with the median having a slightly better RMSE but slightly worse R^2. We proceed using the mean value, as this results in slightly less scatter (and less visibly "boxy" results, see Supporting Figs. 5-7).

It is noteworthy how well the Jorgenson et al. (2022) thermometer performs given that unlike P2008 eq33 or Petrelli et al. (2020), it does not contain a term for H_2O in the liquid (a parameter that is often poorly constrained in natural systems). Like Putirka et al. (2003) there is a correlation between the discrepancy between calculated and experimental temperature and H_2O, but the R^2 value and gradient is smaller (R^2=0.12 vs. 0.33, Grad=-7.33 vs. -10.47°C/1 wt% H_2O, Supporting Fig. 4b).

Interestingly, the Cpx-saturation thermometer of P2008 (eq34), which only uses the liquid composition, also performs well when iterated with Neave and Putirka (2017), having only a slightly higher RMSE and MAE than eq33, but a gradient closer to 1 (0.99), and a very low intercept (29.9°C, Fig. 8b). The similar performance of eq33 and eq34 raises an interesting question as to how much the temperature calculated with a Cpx-Liq thermometer is sensitive to the Cpx composition, or whether the liquid composition is dominating. Petrelli et al. (2020) examine the relative feature importance of each oxide in their machine learning model, showing that for Cpx-Liq temperatures, the three dominant features are MgO, CaO and H_2O in the liquid. We examine the relative importance of the Cpx vs. Liq term for eq33 of P2008 by pairing each experimental liquid with each of the N=214 Cpx in our filtered dataset. For each liquid, we compare the temperatures obtained from each Cpx to the temperature obtained from the true experimental Cpx. While the range of experimental temperatures varies by 350°C, the temperature only changes by ~±50°C based on the Cpx composition (Supporting Fig. 8). Thus, users should be aware when performing Cpx-Liq thermometry that the thermometer is mostly tracking information on the provided liquid composition, not the Cpx (see also Fig. 2d of Till et al., 2012) . The lack of temperature information help by Cpx is also apparent from the poor performance of Cpx-only thermometers (see Section 3.2). The importance of the liquid for temperature also emphasizes the importance of developing reliable equilibrium tests in arc magmas for identifying equilibrium Cpx-Liq pairs.

514

515

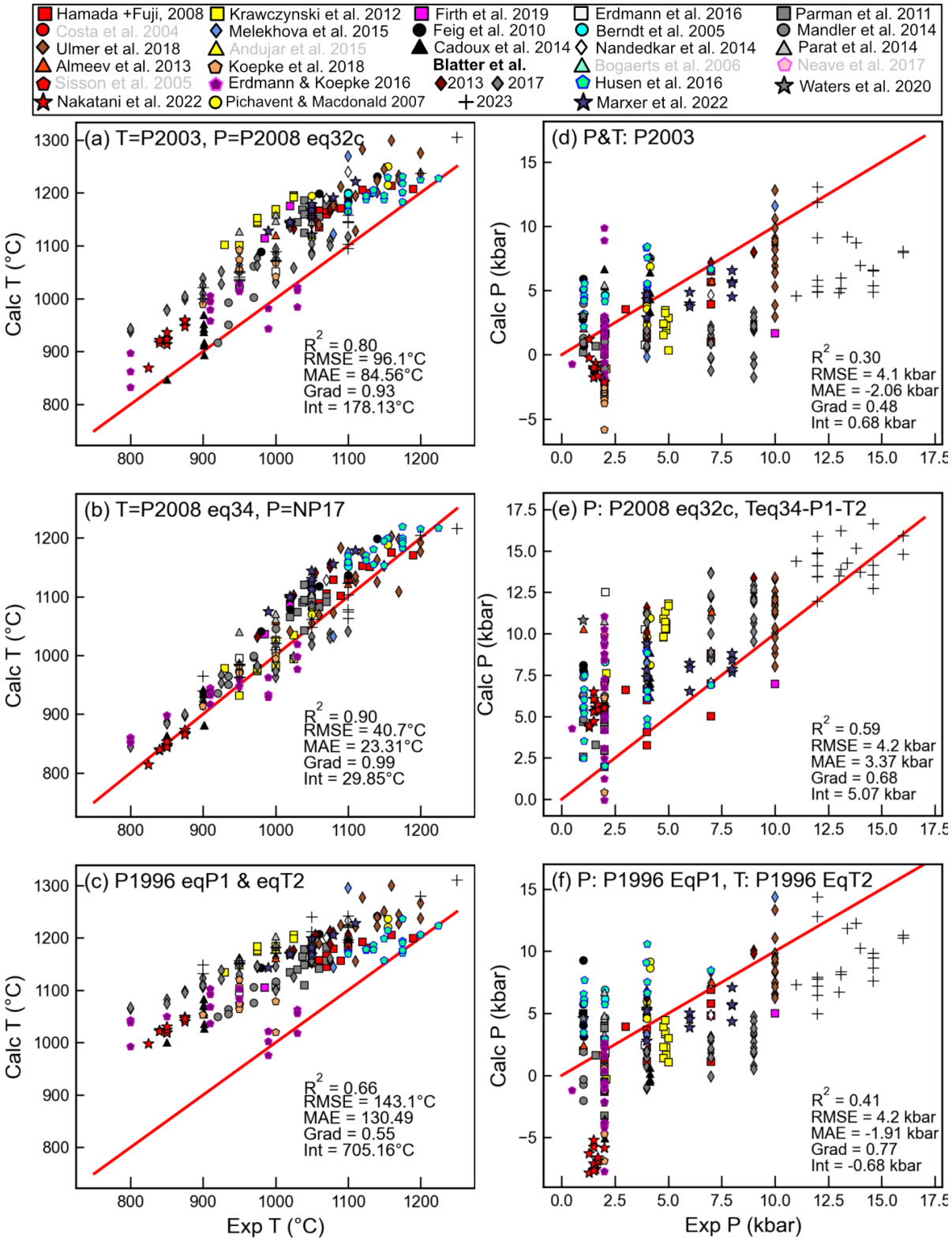
Hamada +Fuji, 2008
Costa et al. 2004
Ulmer et al. 2018
Almeev et al. 2013
Sisson et al. 2005
Nakatani et al. 2022
Krawczynski et al. 2012
Melekhova et al. 2015
Andujar et al. 2015
Koepke et al. 2018
Erdmann & Koepke 2016
Pichavent & Macdonald 2007
Firth et al. 2019
Feig et al. 2010
Cadoux et al. 2014
Blatter et al.
2013 2017
2023
Erdmann et al. 2016
Berndt et al. 2005
Nandedkar et al. 2014
Bogaerts et al. 2006
Husen et al. 2016
Marxer et al. 2022
Parman et al. 2011
Mandler et al. 2014
Parat et al. 2014
Neave et al. 2017
Waters et al. 2020
(a) T=P2003, P=P2008 eq32c
R2 = 0.80
RMSE = 96.1°C
MAE = 84.56°C
Grad = 0.93
Int = 178.13°C
Calc T (°C)
(d) P&T: P2003
R2 = 0.30
RMSE = 4.1 kbar
MAE = -2.06 kbar
Grad = 0.48
Int = 0.68 kbar
Calc P (kbar)
(b) T=P2008 eq34, P=NP17
R2 = 0.90
RMSE = 40.7°C
MAE = 23.31°C
Grad = 0.99
Int = 29.85°C
(e) P: P2008 eq32c, Teq34-P1-T2
R2 = 0.59
RMSE = 4.2 kbar
MAE = 3.37 kbar
Grad = 0.68
Int = 5.07 kbar
(c) P1996 eqP1 & eqT2
R2 = 0.66
RMSE = 143.1°C
MAE = 130.49
Grad = 0.55
Int = 705.16°C
Exp T (°C)
(f) P: P1996 EqP1, T: P1996 EqT2
R2 = 0.41
RMSE = 4.2 kbar
MAE = -1.91 kbar
Grad = 0.77
Int = -0.68 kbar
Exp P (kbar)

516

Fig. 8– Evaluation of various Cpx-Liq thermobarometers (iterating P and T) using experimental water contents for the filtered ArcPL dataset for and temperature (left columns, parts a-c) and pressure (right columns, parts d-f).

Cpx-Liq barometers show substantially worse statistics than thermometers (Fig. 8d-f, Fig. 9). All barometers yield calculated pressures which form a flatter array than the 1:1 line (shown by the gradients <1). The machine-learning barometers of Jorgenson et al. (2022) shows the best performance, closely followed by Petrelli et al. (2020), although these barometers overpredict for low P experiments, as expected for regression tree algorithms. It should be noted that the dataset being used to test the Jorgenson et al. (2022) barometer is slightly different (to avoid overlap with the model calibration dataset). Using the median tree value as suggested by the authors (Supporting Fig. 5a-b) rather than the mean tree results in a substantially lower R^2 value (0.66 vs. 0.74), a higher RMSE (2.5 vs. 2.1 kbar), but a slightly better gradient (0.74 vs. 0.69), and intercept (0.8 vs. 1.7 kbar, Fig. 5). Notably, at the very lowest pressures, the median tree does not experience the overestimation issues to the same degree as the mean tree.

Jorgenson et al. (2022) also suggest that the interquartile range (IQR) of the values returned by all trees for a given Cpx could be used to help filter out poor results in machine-learning-based thermobarometers, which may help improve the performance of their thermobarometers further. They suggest filtering out analyses where the IQR is more than twice the stated RMSE on the thermobarometer. Unfortunately, we find that there is no clear correlation between the discrepancy between experiment and calculated pressure (or temperature), and the IQR of trees (Supporting Fig. 7). This figure also shows there is no correlation between the offset and IQR for the Petrelli et al. (2020) thermobarometers. Thus, at present, it does not seem that applying such a filter is useful. The IQR filter also do not seem to improve statistics for the Cpx-only thermobarometers discussed below (Supporting Fig. 14).

The iterated barometer of Neave and Putirka (2017) with P2008 eq33 thermometer underpredicts P for the vast majority of experiments (Fig. 9a), shown by the strongly negative MAE (-2.12 kbar) and large RMSE (3.9 kbar). P2008 eq31 and eq30 iterated with eq33 show similar performance to one another, with both having relatively low gradients and high intercepts (eq30, Grad=0.52, Int=2.11, Fig. 9b, eq31, Grad=0.58, Int=3.39, Fig. 9c). Thus, they both will overestimate the pressures of low P Cpx, and underestimate for high P Cpx. Putirka (2003, Fig. 8d) forms a very scattered cloud, with similar pressures returned for experiments conducted at 17 and 2 kbar (R^2 is only 0.3, Grad=0.48, RMSE=4.1 kbar). P2008 eq32c using various T estimates (Fig. 8e, Fig. 9d) and P1996 EqP1 and EqT2 (Fig. 8f) also show poor performance.

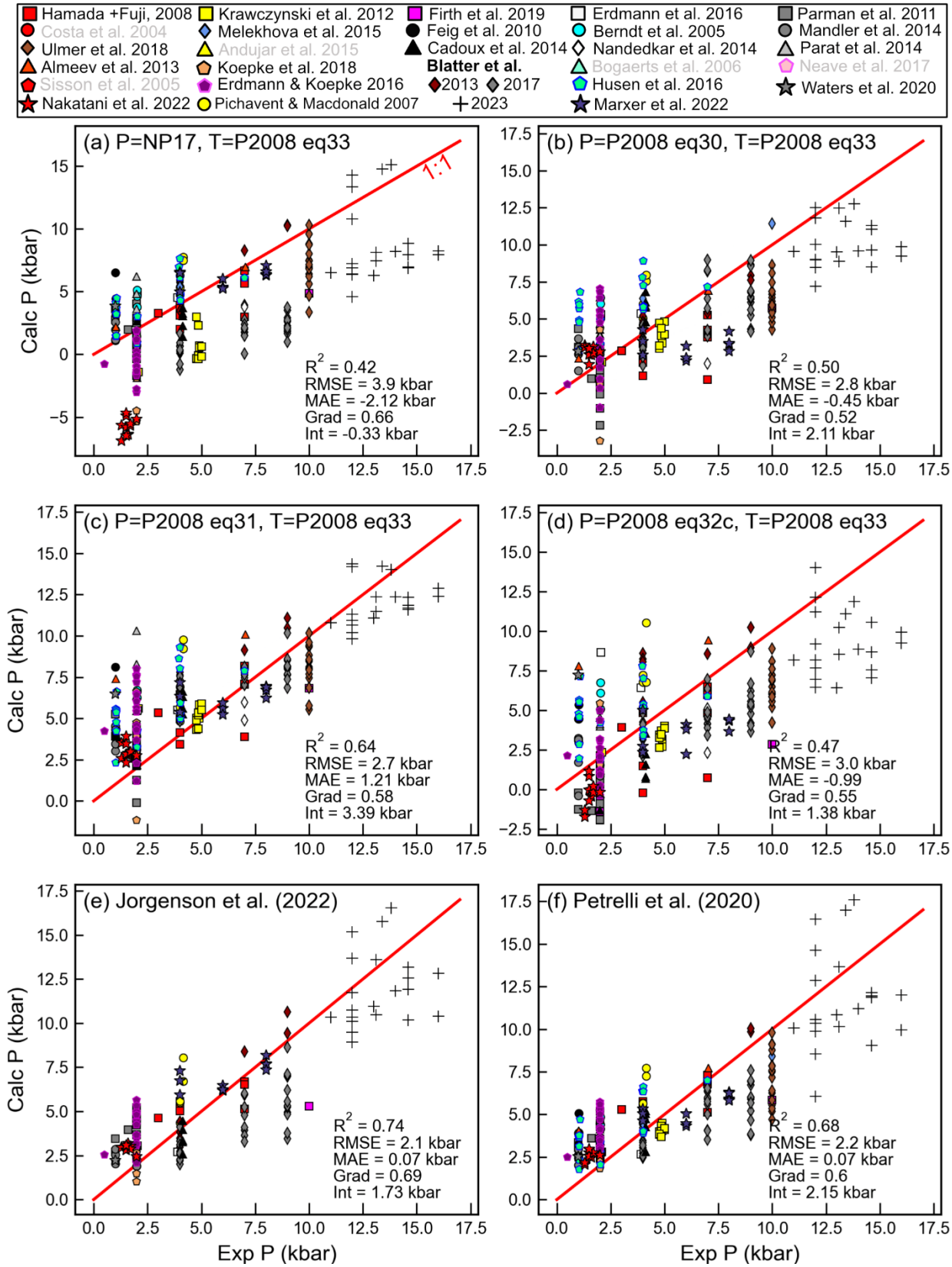

Fig 9 – Evaluation of Cpx-Liq pressures for the filtered ArcPL dataset.

557 *3.1.1. Sensitivity of Cpx-Liq thermobarometry to H_2O*
558 For the comparisons shown in Fig. 7-9, experimental H_2O contents were used when
559 calculations required it. However, in most natural systems, the H_2O content of the melt is
560 highly uncertain, particularly in volcanic systems with no melt inclusion data (e.g., because
561 of a paucity of rapidly-quenched tephra, or at understudied volcanoes). Indeed, the vast
562 majority of Cpx-Liq thermobarometry in arcs has been done using XRF analyses of whole-
563 rock samples. Thus, we investigate how much changing H_2O influences the calculated
564 temperature (Fig. 10) and pressure (Fig. 11), to give insight into the additional sources of
565 uncertainty affecting calculations in variably hydrous arc systems.

566 We randomly select 41 Cpx-Liq pairs from ArcPL. For each of these pairs, we perform
567 calculations at the experimental H_2O, and then perturb H_2O by ±3 wt%, which represents a
568 reasonable uncertainty on the water content of arc systems (where melt inclusion
569 measurements of H_2O generally vary between ~0-6 wt% H_2O; Plank et al., 2013). For each
570 discrete H_2O content, we take the calculated temperature and pressure, and subtract the value
571 calculated using the experimental H_2O content. We do not show results performed using
572 negative water contents. The variation in H_2O for each Cpx-Liq pair is shown as a single line,
573 stretching either side of a black circle showing the experimental H_2O content (where the
574 difference between the perturbed and experimental calculation is 0, Fig. 10-11).

575 Different calibration approaches show different sensitivity to H_2O perturbations. The
576 regression-tree nature of the Cpx-Liq thermometer of Petrelli et al. (2020) means that it
577 exhibits a more complex non-linear sensitivity to H_2O (blue lines, Fig. 10a), where at lower
578 H_2O contents, it is extremely sensitive to H_2O, with temperatures decreasing by as much as
579 70°C for a ~2 wt% increase in H_2O. At higher H_2O contents, calculated temperature changes
580 very little, and in some cases, actually increase with increasing H_2O. P2008 eq33 (using
581 experimental pressures) shows a clear decline in calculated temp with H_2O, with much more
582 similar trends between different samples than for Petrelli et al. (2020, Fig. 10b). When eq33
583 is iterated with P from eq30 instead of using experimental pressures, the temperature still
584 drops (Fig. 10c), but there is a smaller decrease per unit increase in H_2O than in Fig. 10b.
585 There is also a reasonably similar drop with increasing H_2O for eq33 iterated with NP17 (Fig.
586 10d). Excluding Petrelli et al. (2020), an uncertainty in H_2O of only 1 wt% corresponds to an
587 uncertainty in temperature of 10°C.

588

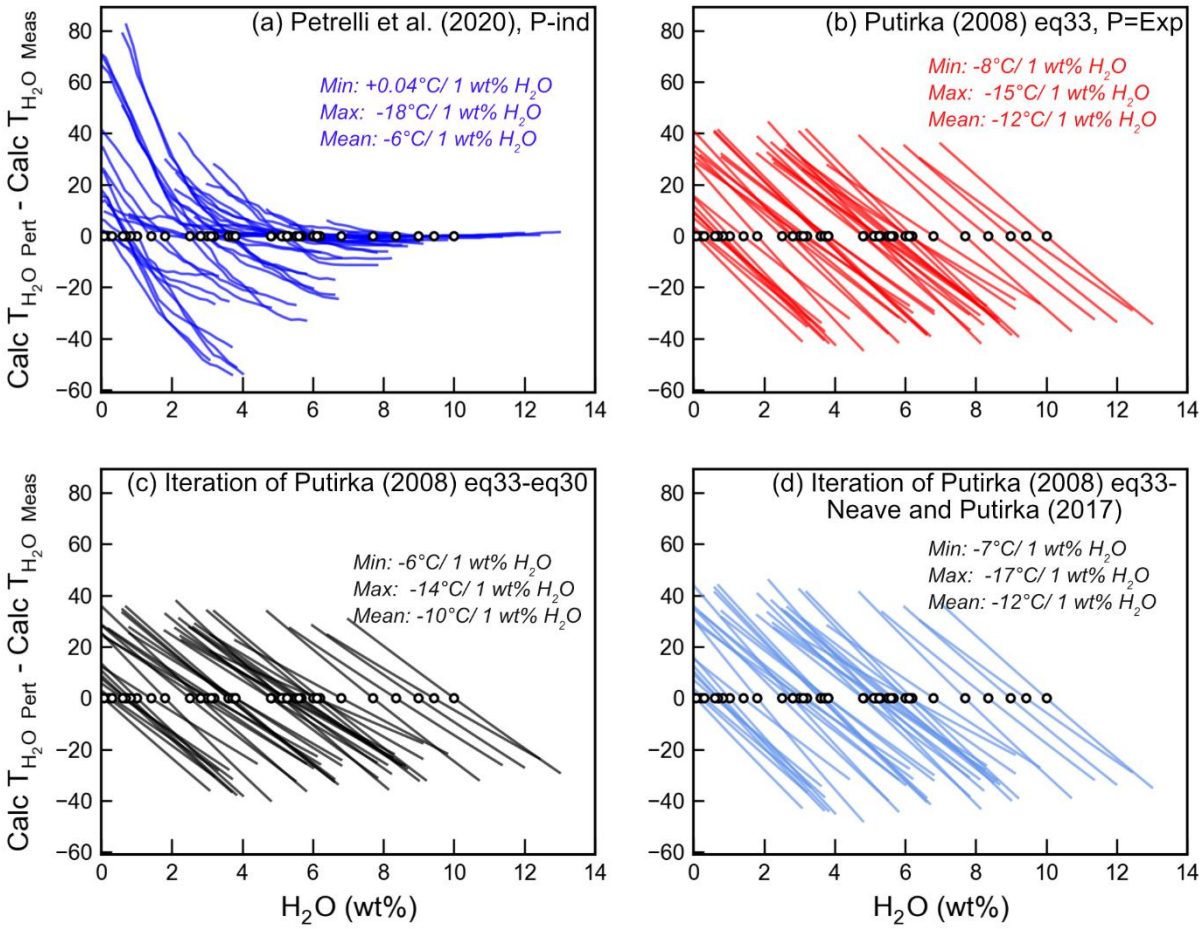

Figure 10 - Sensitivity of calculated temperature to melt H_2O content for 41 randomly selected Cpx-Liq pairs. For each Cpx-Liq pair, we add a linearly-spaced ranging from -3 to +3 to the experimental H_2O content, and calculations are performed for each discrete H_2O value (e.g. for H_2O=4 wt%, calculations are performed from 1-7 wt%). The calculated temperature for the measured H_2O content are subtracted from the calculation for the perturbed H_2O content. This change in temperature for each Cpx-Liq pair is displayed as a colored line, passing through the H_2O content of the experiment (where the T discrepancy is 0). We calculate the max and min change in temperature, and the mean change, for all 41 selected pairs.

Performing the same exercise for Cpx-Liq barometers, we find that Petrelli et al. (2020) shows erratic behaviour, with calculated pressure decreasing with increasing H_2O until ~6 wt%, then increasing again (Fig. 11a). However, the change for all samples is relatively small (<1 kbar). When using experimental temperatures, eq30, eq31, and eq32c show an increase in calculated pressure with increasing H_2O, and all samples show the same gradient (because the H_2O term is multiplied by a constant in each of these equations, Fig. 11b). In contrast, these three barometers show very different behaviour when iterated with eq33, reflecting the fact that temperature and pressure are both affected by H_2O, and they are being iteratively solved (Fig. 11c). In all cases, the change in calculated pressure with changing H_2O for iterative calculations is more subtle than when using experimental temperatures. This is because increasing H_2O decreases the temperature, which decreases the pressure, counteracting the effect of increasing H_2O increasing the pressure. The effect of changing temperature is so

dominant for eq31 that iterative calculations see a decrease in pressure with increasing H_2O (although the effect is relatively subtle). Iteration of eq30 and eq33 is the most sensitive to H_2O, with uncertainty of just 1 wt% in H_2O results in an uncertainty in pressure of 0.26-0.63 kbar. The NP17 barometer has no H_2O term, but iterative calculations using this barometer will be H_2O-sensitive if a H_2O-sensitive thermometer is used (because of the T term in the barometer). Iteration with eq33 results in a relatively small H_2O effect (0.09 kbar per 1 wt% H_2O, Fig. 11d).

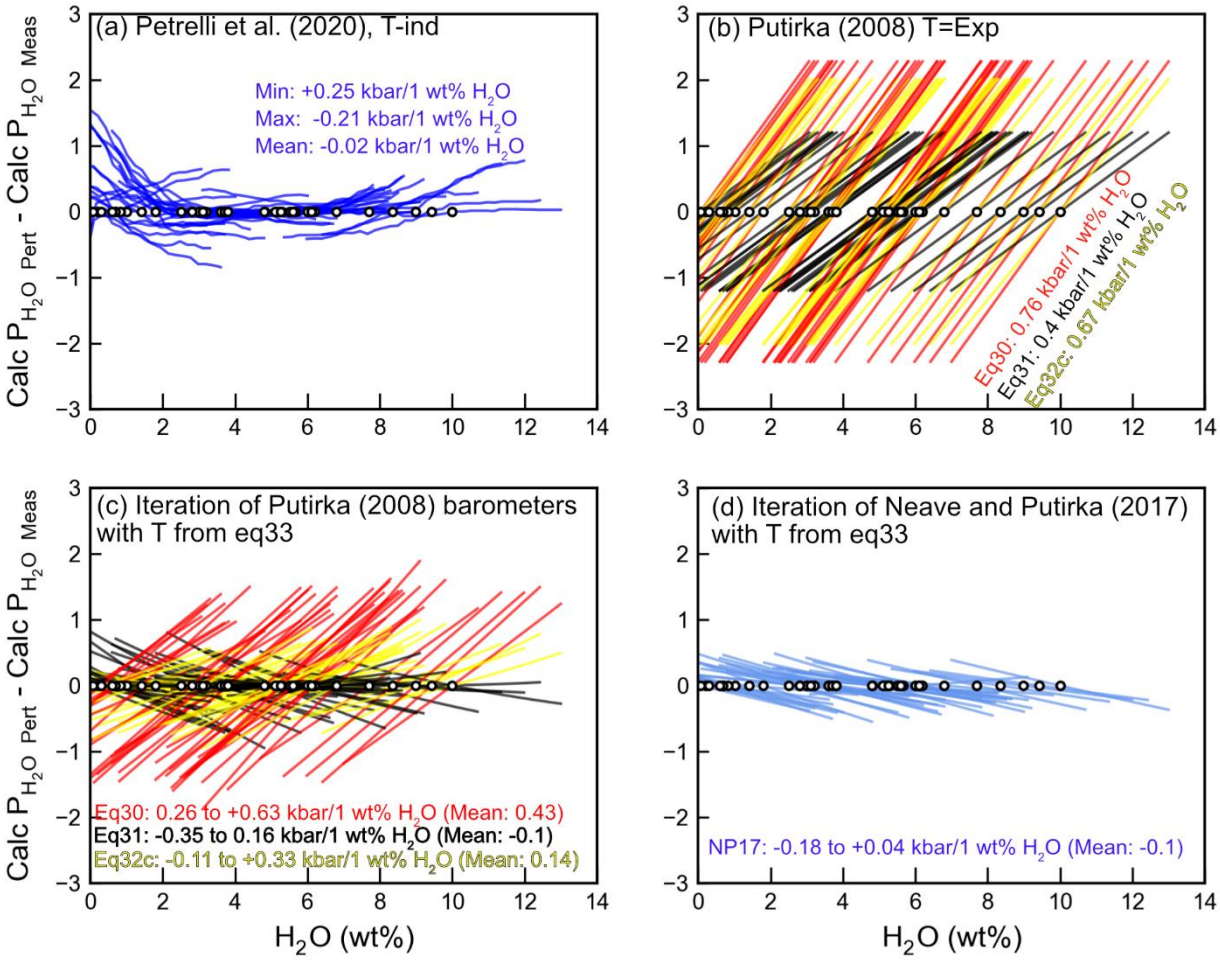

Figure 11 -Using the same method described in Fig. 10, we investigate the sensitivity of calculated pressure to H_2O.

Given that temperature and pressure sensitivity is highly dependent on the choice of equations to iterate, we suggest that in systems where H_2O is not very well constrained, users should propagate uncertainties using methods similar to those here, to assess the possible systematic uncertainty introduced by H_2O terms in equations.

3.2. Assessing suitable Cpx-only thermobarometers

The poor behaviour of many Cpx-Liq equilibrium tests in arc compositions, and the difficulty identifying liquid compositions in arcs where many erupted materials are highly crystalline, means that it would be advantageous to be able to use Cpx-only thermobarometers to deduce

magma storage conditions. We assess the performance of the Cpx-only thermobarometers from Putirka (2008), Petrelli et al. (2020), Jorgenson et al. (2022) and Wang et al. (2021). None of the experiments in our ArcPL test dataset appear in the calibration datasets of Putirka (2008) and Petrelli et al. (2020). Wang et al. (2021) include the experiments of Berndt (2004) and Husen et al. (2016). The calibration dataset of Jorgenson et al. (2022) has substantial overlap with our test dataset (Almeev et al., 2013; Berndt, 2004; Feig et al., 2010; Husen et al., 2016; Krawczynski et al., 2012; Melekhova et al., 2015; Nandedkar et al., 2014; Parat et al., 2014; Ulmer et al., 2018). To obtain the largest possible test dataset here, we exclude these overlapping experiments when testing each thermobarometer only in Fig. 12-13. For fair comparisons between the best barometers in Fig. 15, we only use data that is not in any of the calibration datasets.

Putirka (2008) presents a number of Cpx-only thermobarometers. P2008 eq32d is a P-sensitive, H_2O-independent Cpx-only thermometer. There is also a subsolidus version of eq32d. P2008 eq32a is a T-sensitive barometer which uses only uses the composition of the Cpx, while eq32b also requires users to specify the H_2O content of the liquid. Petrelli et al. (2020) present a Cpx-only barometer calibrated using an extra trees regression (with no H_2O term), but do not present a Cpx-only thermometer. Jorgenson et al. (2022) present a Cpx-only thermometer and barometer, neither of which include a H_2O term. Finally, Wang et al. (2021) present a thermometer (eq2) which has a H_2O term but is P-independent, and a barometer (eq1) which has a T and H_2O term.

When P2008 eq32d (T) is iterated with eq32a or eq32b (P), very similar temperatures are returned regardless of the experimental temperature (Fig. 12a-b, R^2=0.1-0.27, Grad=0.14-0.24). For completeness we also test the subsolidus version of eq32d. This performs slightly better (lower RMSE and MAE), but it greatly underestimates higher temperature experiments (Fig. 12c-d). Putirka (2008) note that eq32d underestimates temperatures in hydrous systems, and indeed we find a correlation between the discrepancy (Exp-Calc T) and H_2O in the liquid (eq32d-32b, R^2=0.47, grad=~-26°C/1 wt%, eq32d-32a: R^2=0.35, grad= ~-20°C/1 wt%, Supporting Fig. 10). Thus, we do not recommend using either of these Cpx-only thermometers in hydrous arc magmas.

The Jorgenson et al. (2022) Cpx-only thermometer also overpredicts (Fig. 12e) for lower temperature experiments, and the discrepancy correlates with H_2O (R^2=0.49, grad= ~-28°C/1 wt%, Supporting Fig. 10). The median and mean of trees show similarly poor performance (Supporting Fig. 11-12).

The Wang et al. (2021) thermometer performs the best (Fig. 12f), which is perhaps unsurprising given that this is the only Cpx-only thermometer which contains a H_2O term. However, it is worth noting that this equation was only calibrated using liquids with SiO_2 contents <60 wt% (e.g., basalts and basaltic-andesites). We find that the discrepancy between the experimental and calculated temperatures increases greatly at higher SiO_2 contents (overpredicting by 200-300°C for the most silicic compositions in our test dataset, Supporting Fig. 13). When only experimental Cpx crystallized in liquids with SiO_2<60 wt% are considered, this thermometer performs much better (Supporting Fig. 13), with an R^2=0.57,

and RMSE=41.6°C. The main problem is that it is difficult to identify from Cpx compositions alone whether a given crystal formed from a liquid with SiO_2>60 wt%. We do not find any robust correlations between Cpx composition and the calculated temperature discrepancy that could be used to apply this filter in natural systems. Thus, the Wang et al. (2021) thermometer needs to be used with extreme care in systems where Cpx may have crystallized from higher SiO_2 liquids. Overall, it is clear from this comparison that Cpx compositions grown from arc magmas do not hold sufficient temperature information without an independent estimate on the melt H_2O content from which they grew. Even when H_2O is included in the regression, Cpx compositions do not result in a very precise or accurate thermometer.

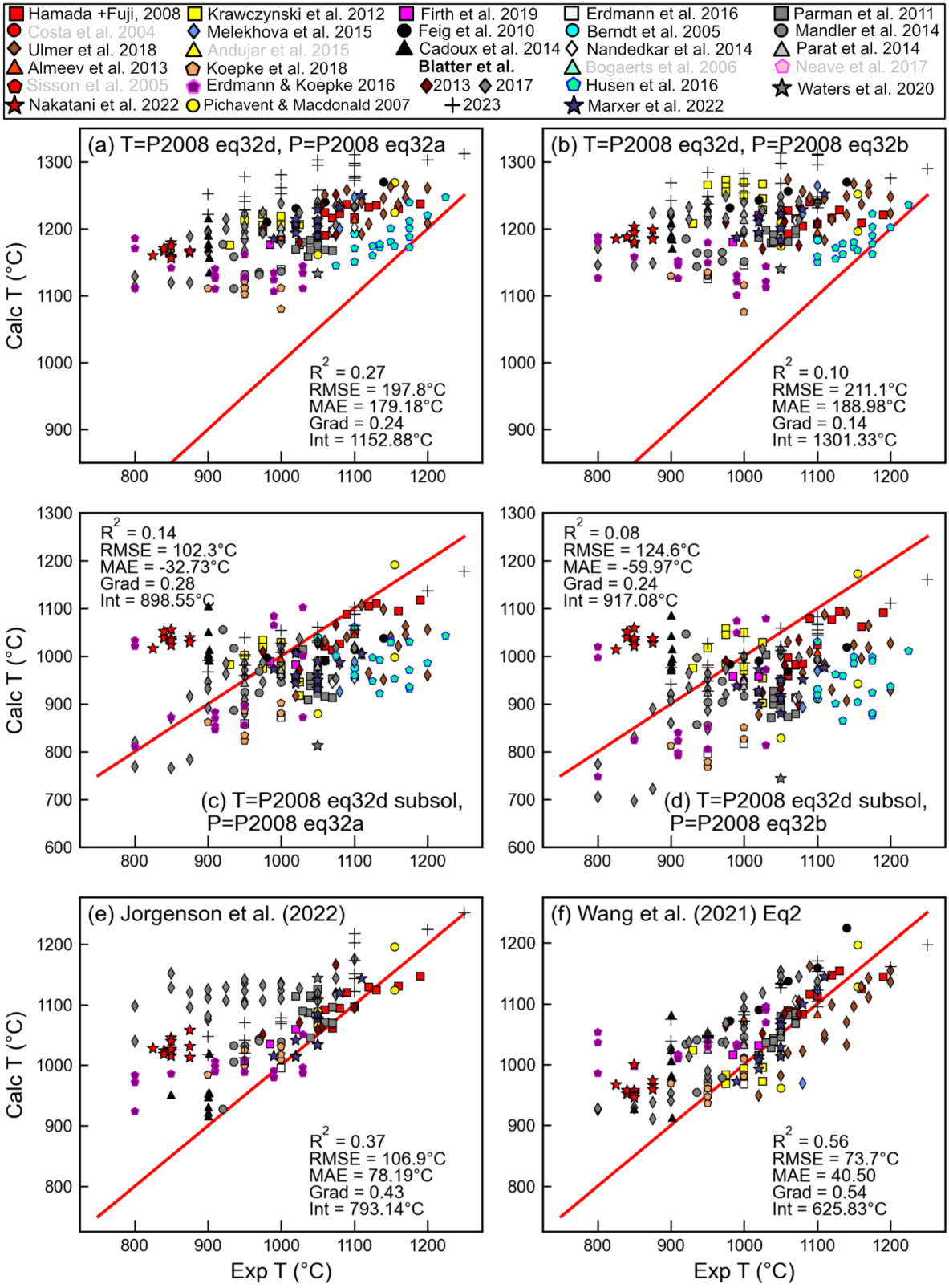

Figure 12 – Comparison of calculated and experimental temperatures for different Cpx-only thermobarometry combinations. For Jorgenson et al. (2022) and Wang et al. (2021), experiments in their calibration dataset are excluded.

Like Cpx-Liq barometers, all Cpx-only barometers have intercepts >0, and gradients <1 (Fig. 13). These non-negative intercepts indicate that all equations overpredict pressure for the lowest pressure experiments (e.g., intercept of 2.4 kbar for eq32d-eq32a, 4 kbar for eq32d-eq32b, and 2 kbar for Petrelli et al. 2020). The Jorgenson et al. (2022) barometer performs the best, with a high gradient (0.8), and a reasonably low intercept (1.1 kbar) and RMSE (1.9 kbar). As for Cpx-Liq, if the median tree is used rather than the mean, the R^2 and RMSE value is worse, but the gradient and intercept slightly better (largely because the median is zero for many low pressure experiments, Supporting Fig. 11). When Petrelli et al. (2020) is applied to the same small dataset used to assess Jorgenson et al. (2022), it is clear Jorgenson et al. (2022) performs slightly better (Fig. 13f vs. g). This is likely because Jorgenson et al. (2022) have more hydrous arc-like magma compositions in their calibration dataset.

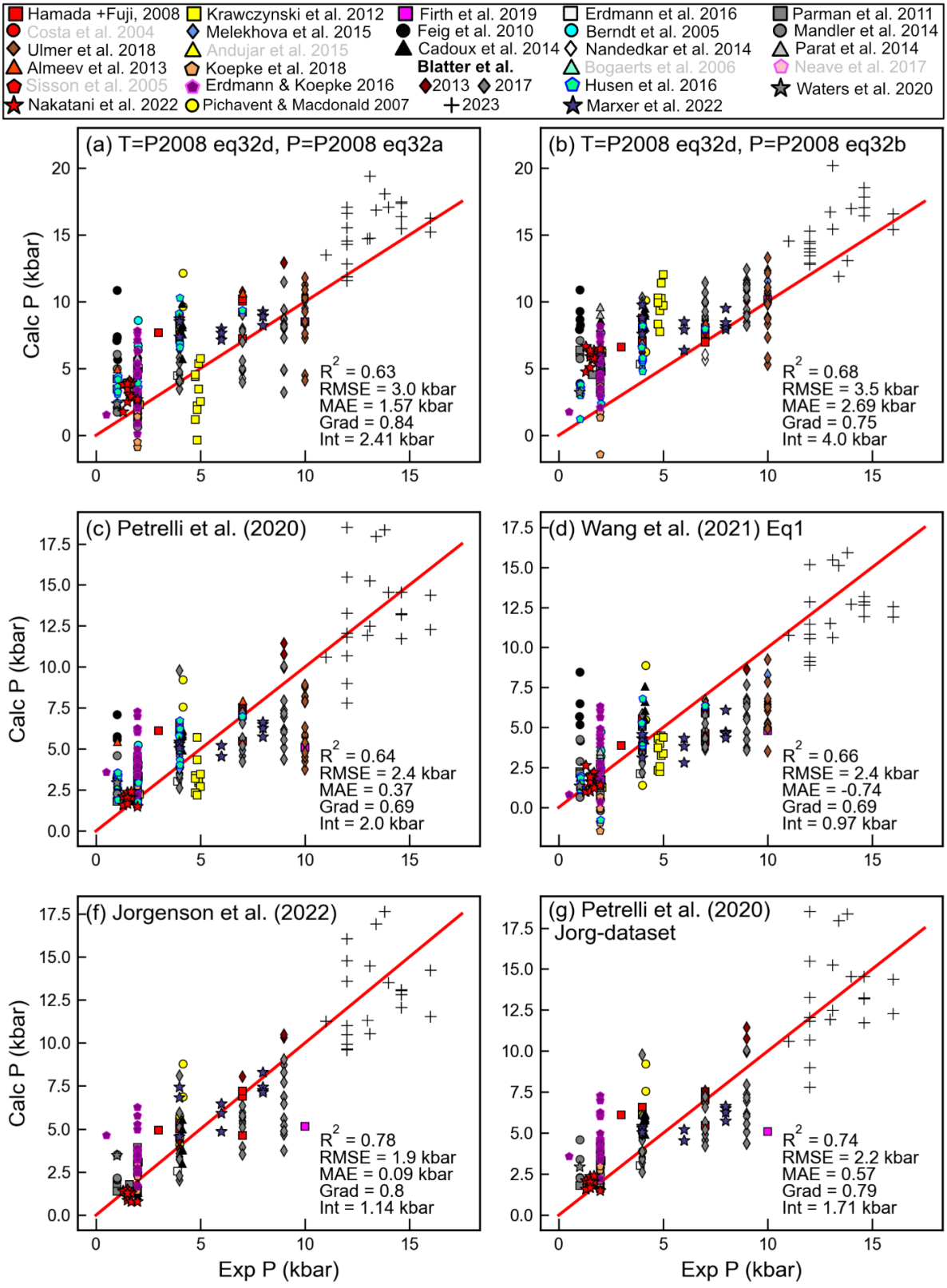

Figure 13 - Assessment of Cpx-only barometers. For Jorgenson et al. (2022) and Wang et al. (2021), experiments in their calibration dataset are excluded.

3.2.1. Sensitivity of Cpx-only thermobarometry to H_2O

It is unlikely that H_2O contents will be precisely known when applying Cpx-only thermobarometry to natural systems (unless melt inclusions in Cpx are analysed). As for Cpx-Liq, we assess the sensitivity of different equation combinations to the melt H_2O contents, to give insights into the additional uncertainties when applying these equations to natural systems. The Wang et al. (2021) 'Cpx-only' thermometer (eq2) is extremely sensitive to H_2O, with calculated temperature decreasing by 23.4°C per 1 wt% H_2O added (Fig. 14a). While eq32d does not have a H_2O term itself, eq32b does, meaning that when these are iterated, calculated temperature actually increases with increasing H_2O (because H_2O changes pressure, which changes temperature). Fortunately, this seemingly spurious effect arising from iteration is quite subtle, with temperature only increasing by ~4-5.6°C per 1 wt% H_2O added (Fig. 14a).

Of the Cpx-only barometers discussed here, only eq32b contains a H_2O term. Calculated pressures increase quite dramatically with added H_2O (mean increase of +0.61 kbar per 1 wt% H_2O, Fig. 14b). This represents an additional source of error when applying this equation in natural systems and should be propagated to obtain an uncertainty estimate. The strong sensitivity to H_2O for some of these equations raises a semantic point of whether these should truly be considered Cpx-only equations. However, the vast majority of studies deploying Cpx-Liq barometry in arc magmas are using whole-rock XRF analyses in place of measured glass compositions, which do not hold any information on H_2O. Thus, it is necessary for studies to estimate the liquid H_2O content to perform calculations (e.g., from melt inclusion analyses in the system of interest, Scruggs and Putirka, 2018), regardless of whether they are using Cpx-Liq or Cpx-only expressions.

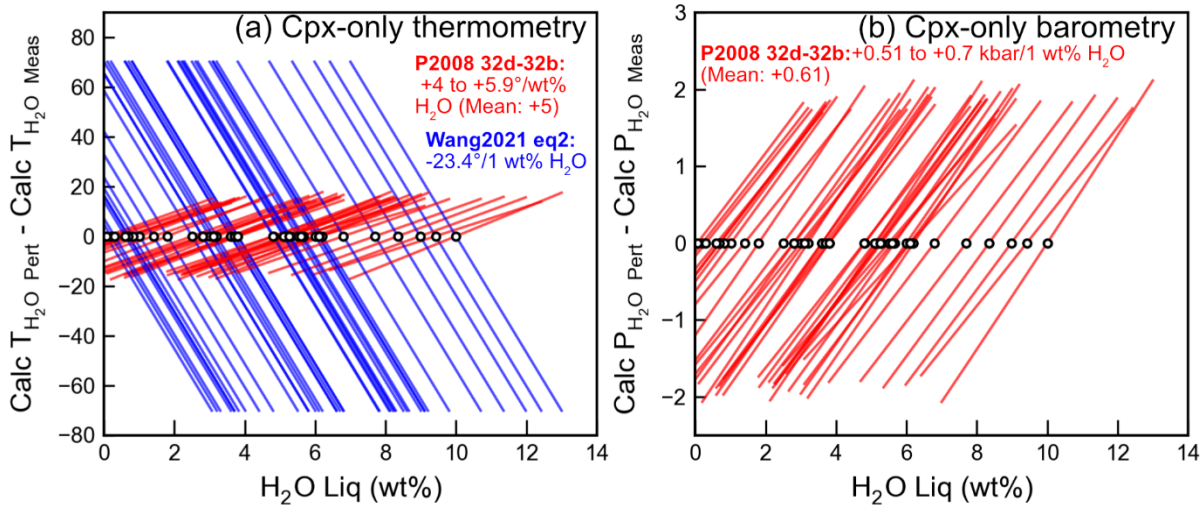

Figure 14 –As for Fig. 10, investigating the sensitivity of Cpx-only pressures and temperatures to H_2O content in the melt.

3.3. What is the resolution of Cpx-based thermobarometry in natural systems?

Our new test dataset shows that if melt H_2O contents are well constrained, Cpx-Liq thermometers can achieve RMSE errors of ~30-40°C, although it should be noted that this is mostly attributed to the temperature information held in the liquid (shown by the similar performance of Liq-only and Cpx-Liq thermometers, and poor performance of Cpx-only thermometers). Fig. 10 also shows the strong sensitivity of the best performing thermometers to melt H_2O contents; uncertainty of just 1 wt% for H_2O contents leads to a systematic uncertainty in temperature of ~8-15°C for the most successful thermometer (eq33, varies with sample and selected barometer). Cpx-only thermometers are inaccurate and imprecise when applied to arc magmas (Fig. 12f), even if melt H_2O is taken into account. The discrepancy between calculated and experimental temperatures is particularly large for low temperature Cpx forming from more silicic melt compositions (>300°C).

Many popular Cpx-Liq and Cpx-only barometers are associated with large systematic and random errors. Systematic error is the reason why many equations have gradients and intercepts substantially different from the 1:1 line when plotted in experimental P vs. Calc P space. These uncertainties may arise from the fact that hydrous experiments are relatively poorly represented in the calibration dataset of many barometers, as well as the regression strategy in the case of tree-based regressions. Sources of random error account in part for large RMSEs and low R^2 values are discussed in detail in Part I of this series (Wieser et al. 2022a). Briefly, Wieser et al. (2022a) suggests that a substantial amount of random error is introduced because of low analytical precision during analyses of minor components such as Na_2O in experimental Cpx. We have attempted to mitigate the effect of this by only using experiments which averaged >5 Cpx measurements, but barometers still show very scattered performance when applied to individual experimental charges. Thus, we investigate whether averaging multiple different experiments conducted at similar pressures can help improve barometer performance, by averaging out sources of random analytical and experimental error (following Putirka et al. 1996).

We show averages for the best behaving Cpx-Liq barometer and Cpx-only barometer (Jorgenson et al. 2022), as well as the second best Cpx-only barometer of Wang et al. (2021). Given their popularity in papers performing thermobarometry in arc magmas, we also show iteration of P2008 eq33 with Neave and Putirka, (2017), iteration of the P and T equations from Putirka (2003) and iteration of P2008 eq33-30 (Table 1, Fig. 15). To compare these thermobarometers, we only use experiments which do not appear in the calibration datasets of any of these six thermobarometers. We round experimental pressures to the nearest 0.2 kbar. Then, for each unique rounded pressure in the dataset, we calculate the total number of Cpx within that pressure 'bin'. For example, at 1 kbar, there are seven different experimental charges, which analysed a total of 65 Cpx (and these experiments could have been conducted from 1.8 to 2.2 kbar). For these seven experimental charges, we calculate the mean and $\pm 1\sigma$ of the calculated pressures and experimental pressures. If more than one experimental charge was present in this pressure bin, we display the average pressure as a red triangle with an error bar (Fig. 15). We calculate statistics for the regression between calculated and predicted pressures in each bin. If only one experimental charge was present in that pressure window,

769 we show a blue triangle (and exclude this datapoint when calculating statistics). A
770 comparable figure using all bin averages to calculate statistics is shown in Supporting Fig. 15.

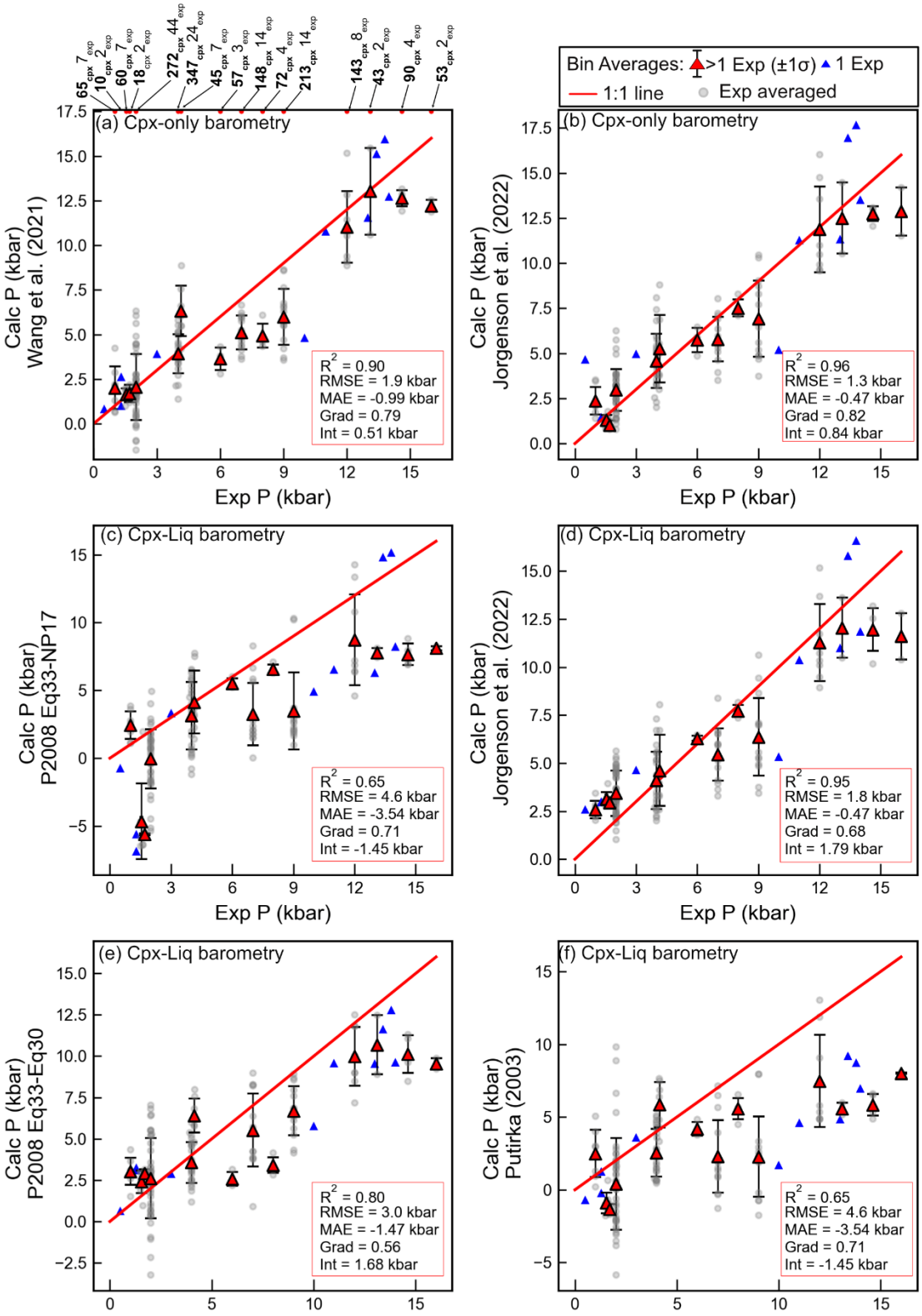

771

Fig 15 – Assessment of effect of averaging on Cpx-only (a-b) and Cpx-Liq barometry (c-f). After rounding experimental pressures to the nearest 0.2 kbar, we average calculated pressures for experiments in the same pressure bin. We show bin averages with >1 experimental charge in red as diamonds, with statistics within the red box. Bins with only 1 experimental charge are shown as blue triangles and not used to calculate statistics. A figure showing statistics for all bins is shown in the supporting information. Experiments averaged for the red triangles are shown as transparent grey symbols. The number of Cpx and number of experimental charges for each bin is indicated in part a).

Averaging multiple experiments yields greatly improved statistics vs. use of only the average Cpx and Glass composition for each experimental charge (compare Fig 15a vs. Fig. 13d, Fig 15b vs. Fig. 13f, Fig. 15c vs. Fig. 9a, Fig. 15d vs. Fig. 9e, see also Putirka et al. 1999). For example, using individual experiments, the Cpx-only barometer of Jorgenson et al. (2022) has a R^2 of 0.78 using individual charges vs. 0.96 when experiments with similar pressures are averaged, and the RMSE reduces from 1.9 kbar to 1.3 kbar. This indicates that significant improvements to Cpx-based barometers could be made if analytical and experimental sources of random uncertainty are mitigated.

While averaging greatly improves the performance of the Cpx-only and Cpx-Liq barometers of Jorgenson et al. (2022), and to a lesser extent Wang et al. (2021), it does not have the same effect on the Cpx-Liq barometers of Neave and Putirka (2017) and Putirka (2003). This indicates that systematic uncertainties are at play in these barometers (which is not improved by averaging). Overall, we suggest that extreme caution should be taken when interpreting published results from the iteration of Neave and Putirka (2017) with eq33 from Putirka (2003) in volcanic arcs, given it substantially underestimates pressures for the dataset tested here.

The improvement following averaging also emphasizes the point of Wieser et al. (2022a) and Putirka et al. (1996) that pressures calculated from individual Cpx are very hard to interpret given the influence of analytical (and/or experimental) uncertainty, but that averages of pressures calculated from large numbers of Cpx may delineate the approximate region of the crust where the crystals grew. However, averaging can be problematic in natural systems, where crystals may have formed at a range of depths, and averaging eliminates true variations. Thus, ultimately it is preferable to obtain higher quality data for individual Cpx analyses in experiments and natural samples than have to rely on averaging which could smear out true variations.

It is interesting that Cpx-only barometers behave just as well, if not slightly better, than Cpx-Liq barometers in the experiments examined here. This suggests that the additional uncertainty and effort associated with identifying equilibrium liquids in natural systems is likely not justified to obtain pressures. However, liquid compositions are certainly required to obtain reliable temperature information, given the poor performance of Cpx-only thermometers.

3.4 Using standard error estimates from thermobarometer calibrations as estimates of uncertainty

Overall, the statistics calculated here using the ArcPL dataset demonstrate that many of the commonly quoted standard error estimates thermobarometers are extremely optimistic, and not representative of the errors associated with the application of these methods in natural systems (where P and T must be iteratively solved, compositions are not the exact ones used to calibrate the model, and H_2O contents are not well known). For example, using P and T calculated from individual experimental charges we calculated a RMSE of 4.1 kbar vs. the often-quoted 1.3 kbar for Putirka (2003, Fig. 8d), and 3.9 kbar vs. 1.4 kbar for Neave and Putirka (2017). RMSEs of 3-4 kbar (equivalent to ~11-15 km for 2700 kg/m^3) translate into a reality where barometers are not able to reliably distinguish storage in the upper, middle and lowermost crust in many volcanic arcs. For example, a 3-4 kbar RMSE values indicates that there is a 67% chance the depth calculated from a given Cpx analysis could have formed anywhere in a ~22-30 km window. Thus, these methods can only pinpoint broad areas of crustal storage. Only after very extensive averaging do the best Cpx-based barometers (Fig. 15, Jorgenson et al. 2022, and Wang et al. 2021) yield RMSEs (1.3 and 1.8 kbar) that permit storage depths to be identified within 10-15 km with 67% confidence. In addition, all these statistics are ideal as they were calculated using known H_2O contents. When applied in nature, the additional uncertainty introduced by using H_2O-sensitive Cpx-only and Cpx-Liq barometers must be propagated and will result in even larger uncertainties.

4. FUTURE DIRECTIONS

The large systematic errors exhibited by many popular Cpx-only thermobarometers and Cpx-Liq barometers in volcanic arcs is disappointing (e.g., Neave and Putirka, 2017, P2008 eq32c, P2008 eq32d-32b, Putirka, 2003) and has implications for published interpretations of magma storage based on these equations. However, given that thermobarometry is often one of the only available petrological tools for investigating magma plumbing system geometries, as many arc volcanoes have no rapidly quenched tephra for melt inclusion work and Amp-only barometry is equally problematic (Erdmann et al., 2014), it is thus critical to find pathways forward. The great improvement in calculated statistics we observe through averaging of multiple experiments conducted at similar pressures suggests that recalibration of Cpx-based barometry based on higher quality experimental data using longer count times for minor elements such as Na, and more analyses per experiment may help to provide a new dataset upon which to recalibrate the next generation of thermobarometers (see Wieser et al. 2022a). This could be based on re-analysis of existing experiments or higher quality analysis of new experiments; higher quality analyses of Cpx in natural and experimental samples will mean that far less averaging is required to reduce scatter in calculated pressures. However, without access to such a high-quality dataset, it is difficult to determine how much improvement this may yield, and whether barometer performance will always be restricted by the relatively weak thermodynamic relationship between mineral components in Cpx and pressure (Putirka, 2008). Given this, extensive averaging of different experiments (and natural Cpx) may still be required.

It is also worth considering that Cpx-based thermobarometry is fundamentally limited by calculating pressure and temperature-sensitive components using EPMA analyses of minerals and melts. Tommasini et al. (2022) examine natural Cpx crystals from Popocat´epetl Volcano and show that mineral components (e.g., Jd) calculated from XRD-informed site assignments differ greatly from the routines used by Neave and Putirka (2017) and P2008 using EPMA data alone. It is very plausible that if the Cpx components could be calculated more precisely and accurately (Tommasini et al., 2022), the performance of thermobarometers would greatly increase.

Additionally, it has been suggested that the presence of Fe^{3+} in Cpx from more oxidised melts stabilizes an aegirine component ($NaFe^{3+}SiO_6$), which convolutes the relationship between pressure and the clinopyroxene Jd component (see Blundy et al., 1995; Neave et al., 2019; Neave and Putirka, 2017 for further discussion). For tholeiitic magmas, Neave et al. (2019) conclude that the aegirine component is not a significant issue and that perhaps Fe^{3+} is incorporated as a Ca-Al-bearing CaFe Tschermak's component. Our dataset, spanning a wider range of fO_2 that of Neave and Putirka (2017) and Neave et al. (2019), shows no clear correlation between the discrepancy between calculated and predicted pressure and the calculated Fe^{3+} proportion in the liquid (from the experimental fO_2), or the proportion of Fe^{3+} predicted in the Cpx using the parameterization in the spreadsheet of Putirka (2008) after Lindsley (1983). However, stoichometric techniques to calculate Fe^{3+} in Cpx are "misleading, inconsistent, and inaccurate" (Dyar et al., 1989), and extremely sensitive to propagated uncertainties from the measurement of other cations (McCanta et al., 2018; Sobolev et al., 1999). While Mössbauer spectroscopy offers high precision detection of Fe^{3+}, it is a bulk analysis method requiring >100 mg of sample, so cannot be applied to the vast majority of experimental products (Rudra, 2021). XANES measurements are challenging, and must take crystal orientation into account because the anisotropy of Cpx to x-ray absorption means orientation must also be taken into account (McCanta et al., 2018; Rudra, 2021). Extensive work determining Fe^{3+} proportions for Cpx in different experimental charges at different redox conditions by XANES, combined with more accurate determination of mineral components, is likely needed to investigate why barometers seem to perform more poorly in arc magmas than tholeiitic magmas (e.g., Neave et al. 2019).

4.1 Calibrating or recalibrating models using this dataset

It would certainly be tempting to recalibrate existing models or develop new models using the ArcPL dataset. However, doing so would mean we no longer have a truly independent test dataset to assess model quality and quantify errors. As a broad generalization, machine-learning researchers encourage a train-test split of ~80:20 or 70:30 (Nguyen et al., 2021), with the default in the popular Python-based machine learning package Sklearn being 75:25. Jorgenson et al. (2022) use their entire dataset of N=2080 Cpx-Liq pairs to calibrate the final model. A new independent dataset to test this would thus require N=520 unique experiments to achieve the Sklearn default ratio. Assessing Cpx-based barometers again after recalibrating using the ArcPL dataset combined with previous datasets would perhaps require waiting another 10-15 years for enough new experiments to be published to re-assess how the newly

calibrated models are performing. Thus, here we choose not to recalibrate models, and instead re-iterate the importance of keeping any test dataset truly isolated during model training and validation. This way, the final 'publishable' model is developed in a way that avoids overconfidence in the model, which can occur when the test dataset has been used at any point during model tuning (Tampu et al., 2022; Wujek et al., 2016).

4. CONCLUSION

Our evaluation of a new dataset of hydrous experiments filtered for K_D and EnFs disequilibrium, cation sums, and number of analyses per experiment, provides new insights into the best thermobarometry calibrations to use when investigating pressures and temperatures in hydrous arc magmas using Cpx-liquid and Cpx alone. We show that the Cpx-Liq thermometers from Petrelli et al. (2020), Jorgenson et al. (2022), and P2008 eq33 all perform well, and can give important insights into magma storage temperatures. However, this work also reveals that the majority of temperature information is stored in the liquid, rather than the Cpx. In contrast, Cpx-only thermometers which do not have a term for H_2O in the liquid perform very poorly indeed, substantially overestimating temperatures for hydrous magmas (e.g., P2008 eq32d, Jorgenson et al. 2022). Only the expression of Wang et al. (2021), which includes a H_2O term, shows a reasonable correspondence between experimental and calculated temperatures, and this expression still performs poorly for Cpx grown in liquids with SiO_2>60 wt%.

Cpx-Liq barometers all behave relatively poorly when applied to individual experimental charges, with large random and systematic errors (all RMSE >2.1, R^2<0.74, Gradient<0.77). Cpx-only barometers are slightly better, but still show relatively large RMSEs (>1.9 kbar), and overpredict at low pressures. Importantly these observed RMSE are all substantially larger than the RMSE reported for many of the calibrations, which are often used as an estimate of uncertainty in studies of natural magmas. While random uncertainties can be addressed by averaging large numbers of Cpx (Fig. 14), even the best performing barometers can only just distinguish between storage zones ~2-3 kbar (or ~ 10 km) apart. Some commonly-used barometers behave extremely poorly, overpredicting pressures by ~4 kbar (Fig. 8e). After averaging, systematic offsets are still very prominent for many barometers. We suggest that additional experimental and analytical work is required to obtain precise (or even accurate) pressures from Cpx compositions in volcanic arcs, to have a large enough high-quality dataset for model calibration and testing without having to perform such extensive averaging (which is hard to translate into natural systems). Given the importance of determining magma storage depths in arcs (Hilley et al., 2022), this should be a key focus of the experimental and petrological community moving forwards.

Acknowledgements

PW thanks helpful conversations with Matt Gleeson, Keith Putirka and Dawnika Blatter (who shared her at-the-time unpublished experimental data). We are greatly for helpful comments from Luca Ziberna, one anonymous reviewer, and editorial handling from Madeleine Humphries. This contribution was supported by funding from National Science Foundation

grants 1948862 and 1949173 to AJRK and CBT, and start-up funds to PW from UC Berkeley.

Data Availability Statement

The excel file containing the new experimental dataset (ArcPL), along with the Jupyter Notebooks used to make every figure can be found on Penny Wieser's GitHub https://github.com/PennyWieser/BarometersBehavingBadly_PartII.

5. REFERENCES

Almeev, R.R., Holtz, F., Ariskin, A.A., Kimura, J.-I., 2013. Storage conditions of Bezymianny Volcano parental magmas: results of phase equilibria experiments at 100 and 700 MPa. Contrib Mineral Petrol 166, 1389–1414. https://doi.org/10.1007/s00410-013-0934-x

Andújar, J., Scaillet, B., Pichavant, M., Druitt, T.H., 2015. Differentiation Conditions of a Basaltic Magma from Santorini, and its Bearing on the Production of Andesite in Arc Settings. Journal of Petrology 56, 765–794. https://doi.org/10.1093/petrology/egv016

Auer, A., White, J., Nakagawa, M., Rosenberg, M., 2013. Petrological record from young Ruapehu eruptions in the 4.5 ka Kiwikiwi Formation, Whangaehu Gorge, New Zealand. New Zealand Journal of Geology and Geophysics 56, 121–133. https://doi.org/10.1080/00288306.2013.796998

Baker, D.R., Eggler, D.H., 1987. Compositions of anhydrous and hydrous melts coexisting with plagioclase, augite, and olivine or low-Ca pyrxene from 1 atm to 8 kbar: Application to the Aleutian volcanic center of Atka. American Mineralogist 72.

Barclay, J., 2004. A Hornblende Basalt from Western Mexico: Water-saturated Phase Relations Constrain a Pressure-Temperature Window of Eruptibility. Journal of Petrology 45, 485–506. https://doi.org/10.1093/petrology/egg091

Bartels, K.S., Kinzler, R.J., Grove, T.L., 1991. High pressure phase relations of primitive high-alumina basalts from Medicine Lake volcano, northern California. Contr. Mineral. and Petrol. 108, 253–270. https://doi.org/10.1007/BF00285935

Belousov, A., Belousova, M., Auer, A., Walter, T.R., Kotenko, T., 2021. Mechanism of the historical and the ongoing Vulcanian eruptions of Ebeko volcano, Northern Kuriles. Bull Volcanol 83, 4. https://doi.org/10.1007/s00445-020-01426-z

Berndt, J., 2004. An Experimental Investigation of the Influence of Water and Oxygen Fugacity on Differentiation of MORB at 200 MPa. Journal of Petrology 46, 135–167. https://doi.org/10.1093/petrology/egh066

Berndt, J., Holtz, F., Koepke, J., 2001. Experimental constraints on storage conditions in the chemically zoned phonolitic magma chamber of the Laacher See volcano. Contrib Mineral Petrol 140, 469–486. https://doi.org/10.1007/PL00007674

Blatter, D.L., Carmichael, I.S.E., 2001. Hydrous phase equilibria of a Mexican high-silica andesite:A candidate for a mantle origin? Geochimica et Cosmochimica Acta 65, 4043–4065. https://doi.org/10.1016/S0016-7037(01)00708-6

Blatter, D.L., Sisson, T.W., Hankins, W.B., 2023. Garnet stability in arc basalt, andesite, and dacite – an experimental study. Contributions to Mineralogy and Petrology.

Blatter, D.L., Sisson, T.W., Hankins, W.B., 2017. Voluminous arc dacites as amphibole reaction-boundary liquids. Contrib Mineral Petrol 172, 27. https://doi.org/10.1007/s00410-017-1340-6

Blatter, D.L., Sisson, T.W., Hankins, W.B., 2013. Crystallization of oxidized, moderately hydrous arc basalt at mid- to lower-crustal pressures: implications for andesite genesis. Contrib Mineral Petrol 166, 861–886. https://doi.org/10.1007/s00410-013-0920-3

Blundy, J.D., Falloon, T.J., Wood, B.J., Dalton, J.A., 1995. Sodium partitioning between clinopyroxene and silicate melts. J. Geophys. Res. 100, 15501–15515. https://doi.org/10.1029/95JB00954

Bogaerts, M., Scaillet, B., Auwera, J.V., 2006. Phase Equilibria of the Lyngdal Granodiorite (Norway): Implications for the Origin of Metaluminous Ferroan Granitoids. Journal of Petrology 47, 2405–2431. https://doi.org/10.1093/petrology/egl049

Brugman, K.K., Till, C.B., 2019. A low-aluminum clinopyroxene-liquid geothermometer for high-silica magmatic systems. American Mineralogist 104, 996–1004. https://doi.org/10.2138/am-2019-6842

Cadoux, A., Scaillet, B., Druitt, T.H., Deloule, E., 2014. Magma Storage Conditions of Large Plinian Eruptions of Santorini Volcano (Greece). Journal of Petrology 55, 1129–1171. https://doi.org/10.1093/petrology/egu021

Carmichael, I.S.E., 1991. The redox states of basic and silicic magmas: a reflection of their source regions? Contr. Mineral. and Petrol. 106, 129–141. https://doi.org/10.1007/BF00306429

Cassidy, M., Watt, S.F.L., Talling, P.J., Palmer, M.R., Edmonds, M., Jutzeler, M., Wall-Palmer, D., Manga, M., Coussens, M., Gernon, T., Taylor, R.N., Michalik, A., Inglis, E., Breitkreuz, C., Le Friant, A., Ishizuka, O., Boudon, G., McCanta, M.C., Adachi, T., Hornbach, M.J., Colas, S.L., Endo, D., Fujinawa, A., Kataoka, K.S., Maeno, F., Tamura, Y., Wang, F., 2015. Rapid onset of mafic magmatism facilitated by volcanic edifice collapse: MAFIC MAGMATISM FACILITATED BY VOLCANIC EDIFICE COLLAPSE. Geophys. Res. Lett. 42, 4778–4785. https://doi.org/10.1002/2015GL064519

Caulfield, J.T., Turner, S.P., Smith, I.E.M., Cooper, L.B., Jenner, G.A., 2012. Magma Evolution in the Primitive, Intra-oceanic Tonga Arc: Petrogenesis of Basaltic Andesites at Tofua Volcano. Journal of Petrology 53, 1197–1230. https://doi.org/10.1093/petrology/egs013

Cigolini, C., Taticchi, T., Alvarado, G.E., Laiolo, M., Coppola, D., 2018. Geological, petrological and geochemical framework of Miravalles-Guayabo caldera and related lavas, NW Costa Rica. Journal of Volcanology and Geothermal Research 358, 207–227. https://doi.org/10.1016/j.jvolgeores.2018.05.013

Costa, F., 2004. Petrological and Experimental Constraints on the Pre-eruption Conditions of Holocene Dacite from Volcan San Pedro (36 S, Chilean Andes) and the Importance of Sulphur in Silicic Subduction-related Magmas. Journal of Petrology 45, 855–881. https://doi.org/10.1093/petrology/egg114

Dahren, B., Troll, V.R., Andersson, U.B., Chadwick, J.P., Gardner, M.F., Jaxybulatov, K., Koulakov, I., 2012. Magma plumbing beneath Anak Krakatau volcano, Indonesia: evidence for multiple magma storage regions. Contrib Mineral Petrol 163, 631–651. https://doi.org/10.1007/s00410-011-0690-8

Deegan, F.M., Whitehouse, M.J., Troll, V.R., Budd, D.A., Harris, C., Geiger, H., Hålenius, U., 2016. Pyroxene standards for SIMS oxygen isotope analysis and their application to Merapi volcano, Sunda arc, Indonesia. Chemical Geology 447, 1–10. https://doi.org/10.1016/j.chemgeo.2016.10.018

Di Carlo, I., 2006. Experimental Crystallization of a High-K Arc Basalt: the Golden Pumice, Stromboli Volcano (Italy). Journal of Petrology 47, 1317–1343. https://doi.org/10.1093/petrology/egl011

Draper, D.S., Johnston, A.D., 1992. Anhydrous PT phase relations of an Aleutian high-MgO basalt: an investigation of the role of olivine-liquid reaction in the generation of arc high-alumina basalts. Contr. Mineral. and Petrol. 112, 501–519. https://doi.org/10.1007/BF00310781

Dyar, M.D., McGuire, J., Ziegler, R., 1989. Redox equilibria and crystal chemistry of coexisting minerals from spinel lherzolite mantle xenoliths. American Mineralogist 74, 969–980.

Erdmann, M., Koepke, J., 2016. Silica-rich lavas in the oceanic crust: experimental evidence for fractional crystallization under low water activity. Contrib Mineral Petrol 171, 83. https://doi.org/10.1007/s00410-016-1294-0

Erdmann, S., Martel, C., Pichavant, M., Bourdier, J.-L., Champallier, R., Komorowski, J.-C., Cholik, N., 2016. Constraints from Phase Equilibrium Experiments on Pre-eruptive Storage Conditions in Mixed Magma Systems: a Case Study on Crystal-rich Basaltic Andesites from Mount Merapi, Indonesia. J. Petrology 57, 535–560. https://doi.org/10.1093/petrology/egw019

Erdmann, S., Martel, C., Pichavant, M., Kushnir, A., 2014. Amphibole as an archivist of magmatic crystallization conditions: problems, potential, and implications for inferring magma storage prior to the paroxysmal 2010 eruption of Mount Merapi, Indonesia. Contrib Mineral Petrol 167, 1016. https://doi.org/10.1007/s00410-014-1016-4

Feig, S.T., Koepke, J., Snow, J.E., 2010. Effect of oxygen fugacity and water on phase equilibria of a hydrous tholeiitic basalt. Contrib Mineral Petrol 160, 551–568. https://doi.org/10.1007/s00410-010-0493-3

Feig, S.T., Koepke, J., Snow, J.E., 2006. Effect of water on tholeiitic basalt phase equilibria: an experimental study under oxidizing conditions. Contrib Mineral Petrol 152, 611–638. https://doi.org/10.1007/s00410-006-0123-2

Firth, C., Adam, J., Turner, S., Rushmer, T., Brens, R., Green, T.H., Erdmann, S., O'Neill, H., 2019. Experimental constraints on the differentiation of low-alkali magmas beneath the Tonga arc: Implications for the origin of arc tholeiites. Lithos 344–345, 440–451. https://doi.org/10.1016/j.lithos.2019.07.008

Freundt, A., Kutterolf, S., 2019. The long-lived Chiltepe volcanic complex, Nicaragua: magmatic evolution at an arc offset. Bull Volcanol 81, 60. https://doi.org/10.1007/s00445-019-1321-x

Gaetani, G.A., Grove, T.L., 1998. The influence of water on melting of mantle peridotite. Contributions to Mineralogy and Petrology 131, 323–346. https://doi.org/10.1007/s004100050396

Geiger, H., Troll, V.R., Jolis, E.M., Deegan, F.M., Harris, C., Hilton, D.R., Freda, C., 2018. Multi-level magma plumbing at Agung and Batur volcanoes increases risk of hazardous eruptions. Sci Rep 8, 10547. https://doi.org/10.1038/s41598-018-28125-2

Ghiorso, M.S., Gualda, G.A.R., 2015. An H2O–CO2 mixed fluid saturation model compatible with rhyolite-MELTS. Contrib Mineral Petrol 169, 53. https://doi.org/10.1007/s00410-015-1141-8

Gleeson, M.L.M., Gibson, S.A., Stock, M.J., 2021. Upper Mantle Mush Zones beneath Low Melt Flux Ocean Island Volcanoes: Insights from Isla Floreana, Galápagos. Journal of Petrology 61, egaa094. https://doi.org/10.1093/petrology/egaa094

Grove, T.L., Donnelly-Nolan, J.M., Housh, T., 1997. Magmatic processes that generated the rhyolite of Glass Mountain, Medicine Lake volcano, N. California. Contributions to Mineralogy and Petrology 127, 205–223. https://doi.org/10.1007/s004100050276

Grove, T.L., Elkins-Tanton, L.T., Parman, S.W., Chatterjee, N., M□ntener, O., Gaetani, G.A., 2003. Fractional crystallization and mantle-melting controls on calc-alkaline differentiation trends.

Contributions to Mineralogy and Petrology 145, 515–533. https://doi.org/10.1007/s00410-003-0448-z

Grove, T.L., Gerlach, D.C., Sando, T.W., 1982. Origin of calc-alkaline series lavas at Medicine Lake Volcano by fractionation, assimilation and mixing. Contr. Mineral. and Petrol. 80, 160–182. https://doi.org/10.1007/BF00374893

Hamada, M., Fujii, T., 2008. Experimental constraints on the effects of pressure and H2O on the fractional crystallization of high-Mg island arc basalt. Contrib Mineral Petrol 155, 767–790. https://doi.org/10.1007/s00410-007-0269-6

Hammer, J., Jacob, S., Welsch, B., Hellebrand, E., Sinton, J., 2016. Clinopyroxene in postshield Haleakala ankaramite: 1. Efficacy of thermobarometry. Contrib Mineral Petrol 171, 7. https://doi.org/10.1007/s00410-015-1212-x

Hesse, M., Grove, T.L., 2003. Absarokites from the western Mexican Volcanic Belt: constraints on mantle wedge conditions. Contributions to Mineralogy and Petrology 146, 10–27. https://doi.org/10.1007/s00410-003-0489-3

Hilley, G. E. (ed.), Brodsky, E.E., Roman, D., Shillington, D. J., Brudzinski, M., Behn, M., Tobin, H. and the SZ4D RCN (2022). SZ4D Implementation Plan. Stanford Digital Repository. https://doi.org/10.25740/HY589FC7561

Hirschmann, M.M., Ghiorso, M.S., Davis, F.A., Gordon, S.M., Mukherjee, S., Grove, T.L., Krawczynski, M., Medard, E., Till, C.B., 2008. Library of Experimental Phase Relations (LEPR): A database and Web portal for experimental magmatic phase equilibria data: LIBRARY OF EXPERIMENTAL PHASE RELATIONS. Geochem. Geophys. Geosyst. 9, n/a-n/a. https://doi.org/10.1029/2007GC001894

Hollyday, A.E., Leiter, S.H., Walowski, K.J., 2020. Pre-eruptive storage, evolution, and ascent timescales of a high-Mg basaltic andesite in the southern Cascade Arc. Contrib Mineral Petrol 175, 88. https://doi.org/10.1007/s00410-020-01730-z

Husen, A., Almeev, R.R., Holtz, F., 2016. The Effect of H2O and Pressure on Multiple Saturation and Liquid Lines of Descent in Basalt from the Shatsky Rise. Journal of Petrology 57, 309–344. https://doi.org/10.1093/petrology/egw008

Iacovino, K., Matthews, S., Wieser, P.E., Moore, G., Begue, F., 2021. VESIcal Part I: An open-source thermodynamic model engine for mixed volatile (H2O-CO2) solubility in silicate melt. Earth and Space Science. https://doi.org/10.1029/2020EA001584

Jeffery, A.J., Gertisser, R., Troll, V.R., Jolis, E.M., Dahren, B., Harris, C., Tindle, A.G., Preece, K., O'Driscoll, B., Humaida, H., Chadwick, J.P., 2013. The pre-eruptive magma plumbing system of the 2007–2008 dome-forming eruption of Kelut volcano, East Java, Indonesia. Contrib Mineral Petrol 166, 275–308. https://doi.org/10.1007/s00410-013-0875-4

Jorgenson, C., Higgins, O., Petrelli, M., Bégué, F., Caricchi, L., 2022. A Machine Learning-Based Approach to Clinopyroxene Thermobarometry: Model Optimization and Distribution for Use in Earth Sciences. JGR Solid Earth 127. https://doi.org/10.1029/2021JB022904

Kawamoto, T., 1996. Experimental constraints on differentiation and H2O abundance of calc-alkaline magmas. Earth and Planetary Science Letters 144, 577–589. https://doi.org/10.1016/S0012-821X(96)00182-3

Kelley, K.A., Cottrell, E., 2009. Water and the Oxidation State of Subduction Zone Magmas. Science 325, 605–607. https://doi.org/10.1126/science.1174156

Koepke, J., Botcharnikov, R.E., Natland, J.H., 2018. Crystallization of late-stage MORB under varying water activities and redox conditions: Implications for the formation of highly evolved lavas

and oxide gabbro in the ocean crust. Lithos 323, 58–77. https://doi.org/10.1016/j.lithos.2018.10.001

Krawczynski, M.J., Grove, T.L., Behrens, H., 2012. Amphibole stability in primitive arc magmas: effects of temperature, H2O content, and oxygen fugacity. Contrib Mineral Petrol 164, 317–339. https://doi.org/10.1007/s00410-012-0740-x

Kress, V.C., Carmichael, I.S.E., 1988. Stoichiometry of the iron oxidation reaction in silicate melts. American Mineralogist.

Lai, Z., Zhao, G., Han, Z., Huang, B., Li, M., Tian, L., Liu, B., Bu, X., 2018. The magma plumbing system in the Mariana Trough back-arc basin at 18° N. Journal of Marine Systems 180, 132–139. https://doi.org/10.1016/j.jmarsys.2016.11.008

Lindsley, D.H., 1983. Pyroxene thermometry. American Mineralogist 68 (5–6), 477–493.

Lormand, C., Zellmer, G.F., Kilgour, G.N., Németh, K., Palmer, A.S., Sakamoto, N., Yurimoto, H., Kuritani, T., Iizuka, Y., Moebis, A., 2021. Slow Ascent of Unusually Hot Intermediate Magmas Triggering Strombolian to Sub-Plinian Eruptions. Journal of Petrology 61, egaa077. https://doi.org/10.1093/petrology/egaa077

Mandler, B.E., Donnelly-Nolan, J.M., Grove, T.L., 2014. Straddling the tholeiitic/calc-alkaline transition: the effects of modest amounts of water on magmatic differentiation at Newberry Volcano, Oregon. Contrib Mineral Petrol 168, 1066. https://doi.org/10.1007/s00410-014-1066-7

Martel, C., Pichavant, M., Holtz, F., Scaillet, B., Bourdier, J.-L., Traineau, H., 1999. Effects of f_{O2} and H_2O on andesite phase relations between 2 and 4 kbar. J. Geophys. Res. 104, 29453–29470. https://doi.org/10.1029/1999JB900191

Marxer, F., Ulmer, P., Müntener, O., 2022. Polybaric fractional crystallisation of arc magmas: an experimental study simulating trans-crustal magmatic systems. Contrib Mineral Petrol 177, 3. https://doi.org/10.1007/s00410-021-01856-8

Masotta, M., Keppler, H., Chaudhari, A., 2016. Fluid-melt partitioning of sulfur in differentiated arc magmas and the sulfur yield of explosive volcanic eruptions. Geochimica et Cosmochimica Acta 176, 26–43. https://doi.org/10.1016/j.gca.2015.12.014

McCanta, M.C., Dyar, M.D., Steven, C., Gunter, M., Lanzirotti, A., 2018. IN SITU MEASUREMENTS OF FE3+ IN PYROXENE USING X-RAY ABSORPTION SPECTROSCOPY: USING AN ORIENTED CRYSTAL CALIBRATION TO REFINE GEOTHERMOBAROMETRIC 2.

Melekhova, E., Blundy, J., Robertson, R., Humphreys, M.C.S., 2015. Experimental Evidence for Polybaric Differentiation of Primitive Arc Basalt beneath St. Vincent, Lesser Antilles. Journal of Petrology 56, 161–192. https://doi.org/10.1093/petrology/egu074

Mercer, C.N., Johnston, A.D., 2008. Experimental studies of the P–T–H2O near-liquidus phase relations of basaltic andesite from North Sister Volcano, High Oregon Cascades: constraints on lower-crustal mineral assemblages. Contrib Mineral Petrol 155, 571–592. https://doi.org/10.1007/s00410-007-0259-8

Mollo, S., Putirka, K., Misiti, V., Soligo, M., Scarlato, P., 2013. A new test for equilibrium based on clinopyroxene–melt pairs: Clues on the solidification temperatures of Etnean alkaline melts at post-eruptive conditions. Chemical Geology 352, 92–100. https://doi.org/10.1016/j.chemgeo.2013.05.026

Moore, G., Carmichael, I.S.E., 1998. The hydrous phase equilibria (to 3 kbar) of an andesite and basaltic andesite from western Mexico: constraints on water content and conditions of

phenocryst growth. Contributions to Mineralogy and Petrology 130, 304–319. https://doi.org/10.1007/s004100050367

Moussallam, Y., Médard, E., Georgeais, G., Rose-Koga, E.F., Koga, K.T., Pelletier, B., Bani, P., Shreve, T.L., Grandin, R., Boichu, M., Tari, D., Peters, N., 2021. How to turn off a lava lake? A petrological investigation of the 2018 intra-caldera and submarine eruptions of Ambrym volcano. Bull Volcanol 83, 36. https://doi.org/10.1007/s00445-021-01455-2

Moussallam, Y., Rose-Koga, E.F., Koga, K.T., Médard, E., Bani, P., Devidal, J.-L., Tari, D., 2019. Fast ascent rate during the 2017–2018 Plinian eruption of Ambae (Aoba) volcano: a petrological investigation. Contrib Mineral Petrol 174, 90. https://doi.org/10.1007/s00410-019-1625-z

Nakatani, T., Kudo, T., Suzuki, T., 2022. Experimental Constraints on Magma Storage Conditions of Two Caldera-Forming Eruptions at Towada Volcano, Japan. JGR Solid Earth 127. https://doi.org/10.1029/2021JB023665

Namur, O., Montalbano, S., Bolle, O., Vander Auwera, J., 2020. Petrology of the April 2015 Eruption of Calbuco Volcano, Southern Chile. Journal of Petrology 61, egaa084. https://doi.org/10.1093/petrology/egaa084

Nandedkar, R.H., Ulmer, P., Müntener, O., 2014. Fractional crystallization of primitive, hydrous arc magmas: an experimental study at 0.7 GPa. Contrib Mineral Petrol 167, 1015. https://doi.org/10.1007/s00410-014-1015-5

Neave, D.A., Bali, E., Guðfinnsson, G.H., Halldórsson, S.A., Kahl, M., Schmidt, A.-S., Holtz, F., 2019. Clinopyroxene–Liquid Equilibria and Geothermobarometry in Natural and Experimental Tholeiites: the 2014–2015 Holuhraun Eruption, Iceland. Journal of Petrology 60, 1653–1680. https://doi.org/10.1093/petrology/egz042

Neave, D.A., Putirka, K.D., 2017. A new clinopyroxene-liquid barometer, and implications for magma storage pressures under Icelandic rift zones. American Mineralogist 102, 777–794. https://doi.org/10.2138/am-2017-5968

Nguyen, Q.H., Ly, H.-B., Ho, L.S., Al-Ansari, N., Le, H.V., Tran, V.Q., Prakash, I., Pham, B.T., 2021. Influence of data splitting on performance of machine learning models in prediction of shear strength of soil. Mathematical Problems in Engineering 2021, 1–15.

Nimis, P., 1999. Clinopyroxene geobarometry of magmatic rocks. Part 2. Structural geobarometers for basic to acid, tholeiitic and mildly alkaline magmatic systems. Contrib Mineral Petrol 135, 62–74. https://doi.org/10.1007/s004100050498

Parat, F., Streck, M., Holtz, F., Almeev, R.R., 2014. Experimental study into the petrogenesis of crystal-rich basaltic to andesitic magmas at Arenal volcano. Contributions to Mineralogy and Petrology.

Parman, S.W., Grove, T.L., Kelley, K.A., Plank, T., 2011. Along-Arc Variations in the Pre-Eruptive H2O Contents of Mariana Arc Magmas Inferred from Fractionation Paths. Journal of Petrology 52, 257–278. https://doi.org/10.1093/petrology/egq079

Petrelli, M., Caricchi, L., Perugini, D., 2020. Machine Learning Thermo-Barometry: Application to Clinopyroxene-Bearing Magmas. J. Geophys. Res. Solid Earth 125. https://doi.org/10.1029/2020JB020130

Pichavant, M., Macdonald, R., 2007. Crystallization of primitive basaltic magmas at crustal pressures and genesis of the calc-alkaline igneous suite: experimental evidence from St Vincent, Lesser Antilles arc. Contrib Mineral Petrol 154, 535–558. https://doi.org/10.1007/s00410-007-0208-6

Plank, T., Kelley, K.A., Zimmer, M.M., Hauri, E.H., Wallace, P.J., 2013. Why do mafic arc magmas contain ~4wt% water on average? Earth and Planetary Science Letters 364, 168–179. https://doi.org/10.1016/j.epsl.2012.11.044

Preece, K., Gertisser, R., Barclay, J., Berlo, K., Herd, R.A., 2014. Pre- and syn-eruptive degassing and crystallisation processes of the 2010 and 2006 eruptions of Merapi volcano, Indonesia. Contrib Mineral Petrol 168, 1061. https://doi.org/10.1007/s00410-014-1061-z

Profeta, L., Ducea, M.N., Chapman, J.B., Paterson, S.R., Gonzales, S.M.H., Kirsch, M., Petrescu, L., DeCelles, P.G., 2016. Quantifying crustal thickness over time in magmatic arcs. Sci Rep 5, 17786. https://doi.org/10.1038/srep17786

Putirka, K., 1999. Clinopyroxene + liquid equilibria to 100 kbar and 2450 K. Contributions to Mineralogy and Petrology 135, 151–163. https://doi.org/10.1007/s004100050503

Putirka, K.D., 2008a. Thermometers and Barometers for Volcanic Systems. Reviews in Mineralogy and Geochemistry 69, 61–120. https://doi.org/10.2138/rmg.2008.69.3

Putirka, K.D., 2008b. Thermometers and Barometers for Volcanic Systems. Reviews in Mineralogy and Geochemistry 69, 61–120. https://doi.org/10.2138/rmg.2008.69.3

Putirka, K.D., Mikaelian, H., Ryerson, F., Shaw, H., 2003. New clinopyroxene-liquid thermobarometers for mafic, evolved, and volatile-bearing lava compositions, with applications to lavas from Tibet and the Snake River Plain, Idaho. American Mineralogist 88, 1542–1554. https://doi.org/10.2138/am-2003-1017

Rader, E.L., Larsen, J.F., 2013. Experimental phase relations of a low MgO Aleutian basaltic andesite at XH2O = 0.7–1. Contrib Mineral Petrol 166, 1593–1611. https://doi.org/10.1007/s00410-013-0944-8

Riker, J.M., Blundy, J.D., Rust, A.C., Botcharnikov, R.E., Humphreys, M.C.S., 2015. Experimental phase equilibria of a Mount St. Helens rhyodacite: a framework for interpreting crystallization paths in degassing silicic magmas. Contrib Mineral Petrol 170, 6. https://doi.org/10.1007/s00410-015-1160-5

Romero, J.E., Morgado, E., Pisello, A., Boschetty, F., Petrelli, M., Cáceres, F., Alam, M.A., Polacci, M., Palma, J.L., Arzilli, F., Vera, F., Gutiérrez, R., Morgavi, D., 2022. Pre-eruptive Conditions of the 3 March 2015 Lava Fountain of Villarrica Volcano (Southern Andes). Bull Volcanol 85, 2. https://doi.org/10.1007/s00445-022-01621-0

Rudra, A., 2021. FERRIC IRON PARTITIONING BETWEEN PYROXENE AND MELT: EXPERIMENTS, MICROBEAM ANALYSIS, AND CONSEQUENCES FOR MANTLE REDOX. PhD thesis, University of Minnesota.

Ruth, D.C.S., Costa, F., 2021. A petrological and conceptual model of Mayon volcano (Philippines) as an example of an open-vent volcano. Bull Volcanol 83, 62. https://doi.org/10.1007/s00445-021-01486-9

Rutherford, M.J., Sigurdsson, H., Carey, S., Davis, A., 1985. The May 18, 1980, eruption of Mount St. Helens: 1. Melt composition and experimental phase equilibria. J. Geophys. Res. 90, 2929. https://doi.org/10.1029/JB090iB04p02929

Sas, M., DeBari, S., Clynne, M., Rusk, B., 2017. Using mineral geochemistry to decipher slab, mantle, and crustal input in the generation of high-Mg andesites and basaltic andesites from the northern Cascade Arc. msam. https://doi.org/10.2138/am-2017-5756

Scruggs, M.A., Putirka, K.D., 2018. Eruption triggering by partial crystallization of mafic enclaves at Chaos Crags, Lassen Volcanic Center, California. American Mineralogist 103, 1575–1590. https://doi.org/10.2138/am-2018-6058

Sheehan, F., Barclay, J., 2016. Staged storage and magma convection at Ambrym volcano, Vanuatu. Journal of Volcanology and Geothermal Research 322, 144–157. https://doi.org/10.1016/j.jvolgeores.2016.02.024

Sisson, T.W., Ratajeski, K., Hankins, W.B., Glazner, A.F., 2005. Voluminous granitic magmas from common basaltic sources. Contrib Mineral Petrol 148, 635–661. https://doi.org/10.1007/s00410-004-0632-9

Sobolev, V.N., McCammon, C.A., Taylor, L.A., Snyder, G.A., Sobolev, N.V., 1999. Precise Moessbauer milliprobe determination of ferric iron in rock-forming minerals and limitations of electron microprobe analysis. American Mineralogist 84, 78–85. https://doi.org/10.2138/am-1999-1-208

Solaro, C., Martel, C., Champallier, R., Boudon, G., Balcone-Boissard, H., Pichavant, M., 2019. Petrological and experimental constraints on magma storage for large pumiceous eruptions in Dominica island (Lesser Antilles). Bull Volcanol 81, 55. https://doi.org/10.1007/s00445-019-1313-x

Tampu, I.E., Eklund, A., Haj-Hosseini, N., 2022. Inflation of test accuracy due to data leakage in deep learning-based classification of OCT images. Sci Data 9, 580. https://doi.org/10.1038/s41597-022-01618-6

Till, C.B., Grove, T.L., Krawczynski, M.J., 2012. A melting model for variably depleted and enriched lherzolite in the plagioclase and spinel stability fields: A MODEL FOR MELTING MODIFIED MANTLE. J. Geophys. Res. 117, n/a-n/a. https://doi.org/10.1029/2011JB009044

Tommasini, S., Bindi, L., Savia, L., Mangler, M.F., Orlando, A., Petrone, C.M., 2022. Critical assessment of pressure estimates in volcanic plumbing systems: The case study of Popocatépetl volcano, Mexico. Lithos 408–409, 106540. https://doi.org/10.1016/j.lithos.2021.106540

Ulmer, P., Kaegi, R., Müntener, O., 2018. Experimentally Derived Intermediate to Silica-rich Arc Magmas by Fractional and Equilibrium Crystallization at 1·0 GPa: an Evaluation of Phase Relationships, Compositions, Liquid Lines of Descent and Oxygen Fugacity. Journal of Petrology 59, 11–58. https://doi.org/10.1093/petrology/egy017

Wang, X., Hou, T., Wang, M., Zhang, C., Zhang, Z., Pan, R., Marxer, F., Zhang, H., 2021. A new clinopyroxene thermobarometer for mafic to intermediate magmatic systems. Eur. J. Mineral. 33, 621–637. https://doi.org/10.5194/ejm-33-621-2021

Waters, L.E., Cottrell, E., Coombs, M.L., Kelley, K.A., 2021. Generation of Calc-Alkaline Magmas during Crystallization at High Oxygen Fugacity: An Experimental and Petrologic Study of Tephras from Buldir Volcano, Western Aleutian Arc, Alaska, USA. Journal of Petrology 62, egaa104. https://doi.org/10.1093/petrology/egaa104

Wieser, P., Petrelli, M., Lubbers, J., Wieser, E., Kent, A., Till, C., 2022. Thermobar: An Open-Source Thermobarometry Hygrometry and Chemometer Python 3 Tool. Preprint submitted to EarthArxiv. https://doi.org/10.31223/X5FD0K.

Wieser, P. E., Iacovino, K., Matthews, S., Moore, G., Allison, C.M., 2022. VESIcal: 2. A Critical Approach to Volatile Solubility Modeling Using an Open-Source Python3 Engine. Earth and Space Science 9. https://doi.org/10.1029/2021EA001932

Wieser, P.E., Kent, A., Till, C., Donovan, J., Neave, D., Blatter, D., Mike Krawczynski, M., 2023. Barometers behaving badly: Assessing the influence of analytical and experimental uncertainty on clinopyroxene thermobarometry calculations at crustal conditions (preprint). Earth Sciences. https://doi.org/10.31223/X5JT0N

Wieser, P.E., Petrelli, M., Lubbers, J., Wieser, E., Ozaydin, S., Kent, A., Till, C., 2022. Thermobar: An open-source Python3 tool for thermobarometry and hygrometry. Volcanica 5, 349–384. https://doi.org/10.30909/vol.05.02.349384

Wood, B.J., Blundy, J., 1997. predictive model for rare earth element partitioning between clinopyroxene and anhydrous silicate melt. Contributions to Mineralogy and Petrology.

Wujek, B., Hall, P., Günes, F., 2016. Best practices for machine learning applications. SAS Institute Inc.

Supporting Information for "Barometers behaving badly II: A critical evaluation of Cpx-only and Cpx-Liq thermobarometry in variably-hydrous arc magmas"

Penny E. Wieser[1,2], Adam Kent[2], Christy Till[3]

1. **Corresponding author**: Penny_wieser@berkeley.edu. Department of Earth and Planetary Sciences, McCone Hall, UC Berkeley, 94720, USA
2. College of Earth, Ocean and Atmospheric Sciences, Oregon State University, 97331, USA
3. School of Earth and Space Exploration, Arizona State University, Tempe, AZ 85281, USA

Supporting figures

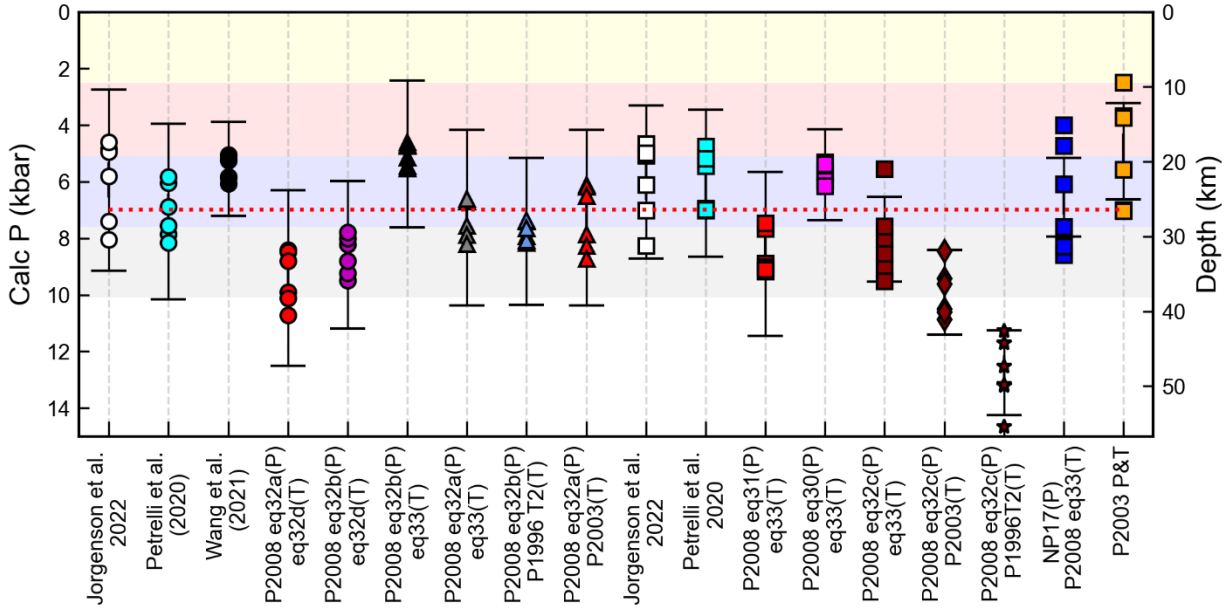

Supporting Fig. 1 – Comparison of different barometers as in Fig. 1a in the main text, but for 7 kbar experiments from Blatter et al. (2013)

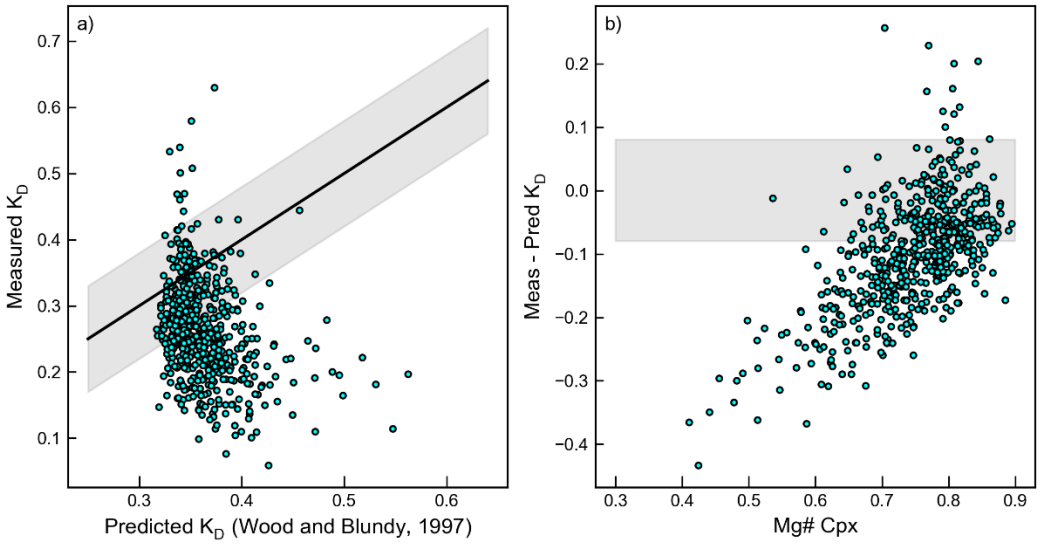

Supporting Fig. 2. Comparison of predicted and measured K_D using Wood and Blundy (1997). There is a clear offset between the measured and predicted K_D value, and the Mg# of the Cpx, with the equation performing very poorly for low Mg# Cpx.

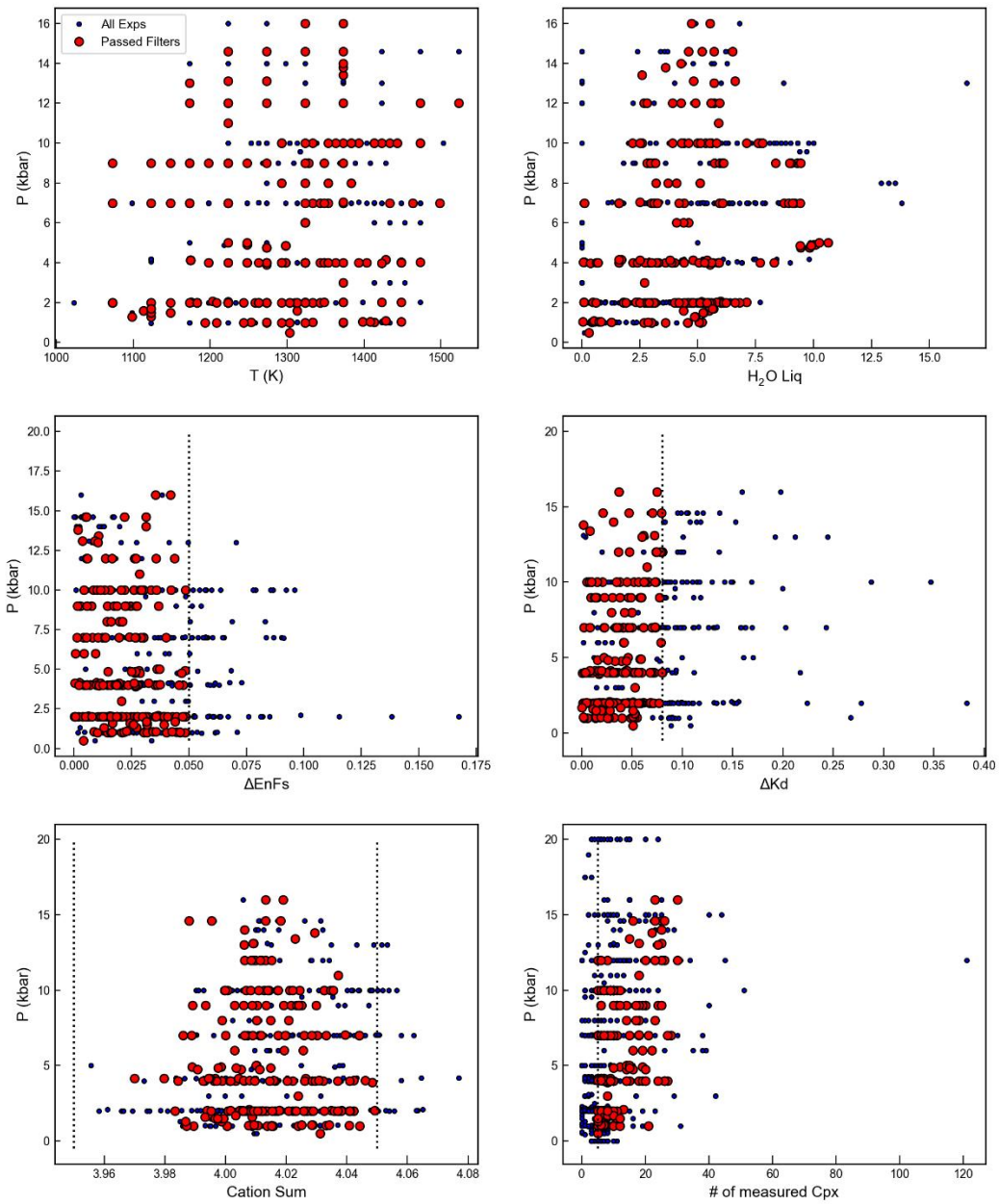
All Exps
Passed Filters
P (kbar)
T (K)
P (kbar)
H2O Liq
P (kbar)
ΔEnFs
P (kbar)
ΔKd
P (kbar)
Cation Sum
P (kbar)
# of measured Cpx

Supporting Fig. 3 – Filters applied to dataset (cut off value indicated with a dashed line). The H_2O filter removes all experiments conducted at atmospheric pressure (none of which have reported water contents).

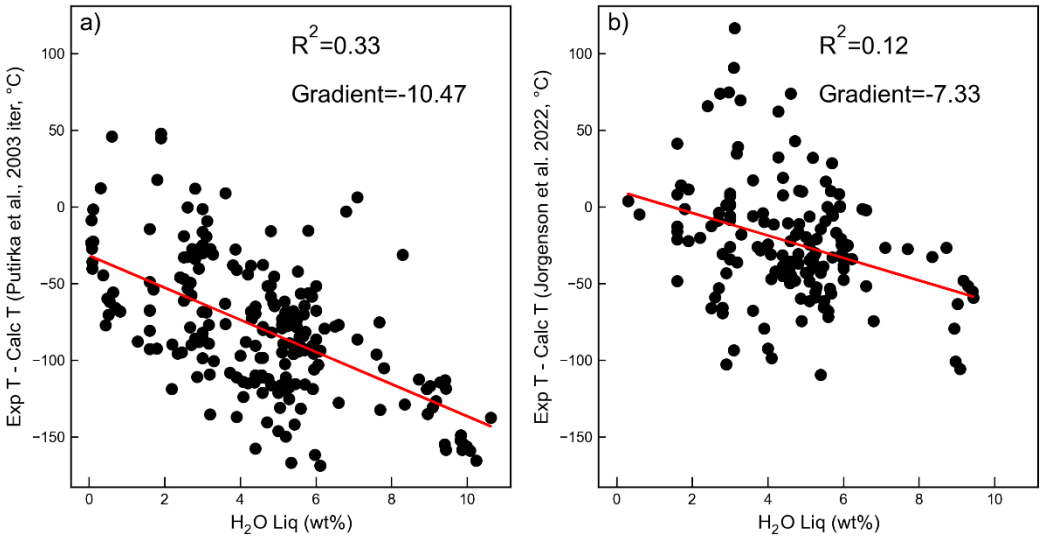

Supporting Fig. 4 – a) The discrepancy between calculated and experimental temperature iterating the thermometer and barometer of Putirka et al. (2003) increases with increasing H_2O content in the liquid. This is not surprising, given this equation has no term for H_2O, but is concerning given this equation is still used for arc magmas (see Table 1 in the main text). b) The Cpx-Liq thermometer of Jorgenson et al. (2022) also doesn't contain a H_2O term. However, the discrepancy between experimental and calculated temperature shows a much less strong correlation with water content (lower R^2, less negative gradient).

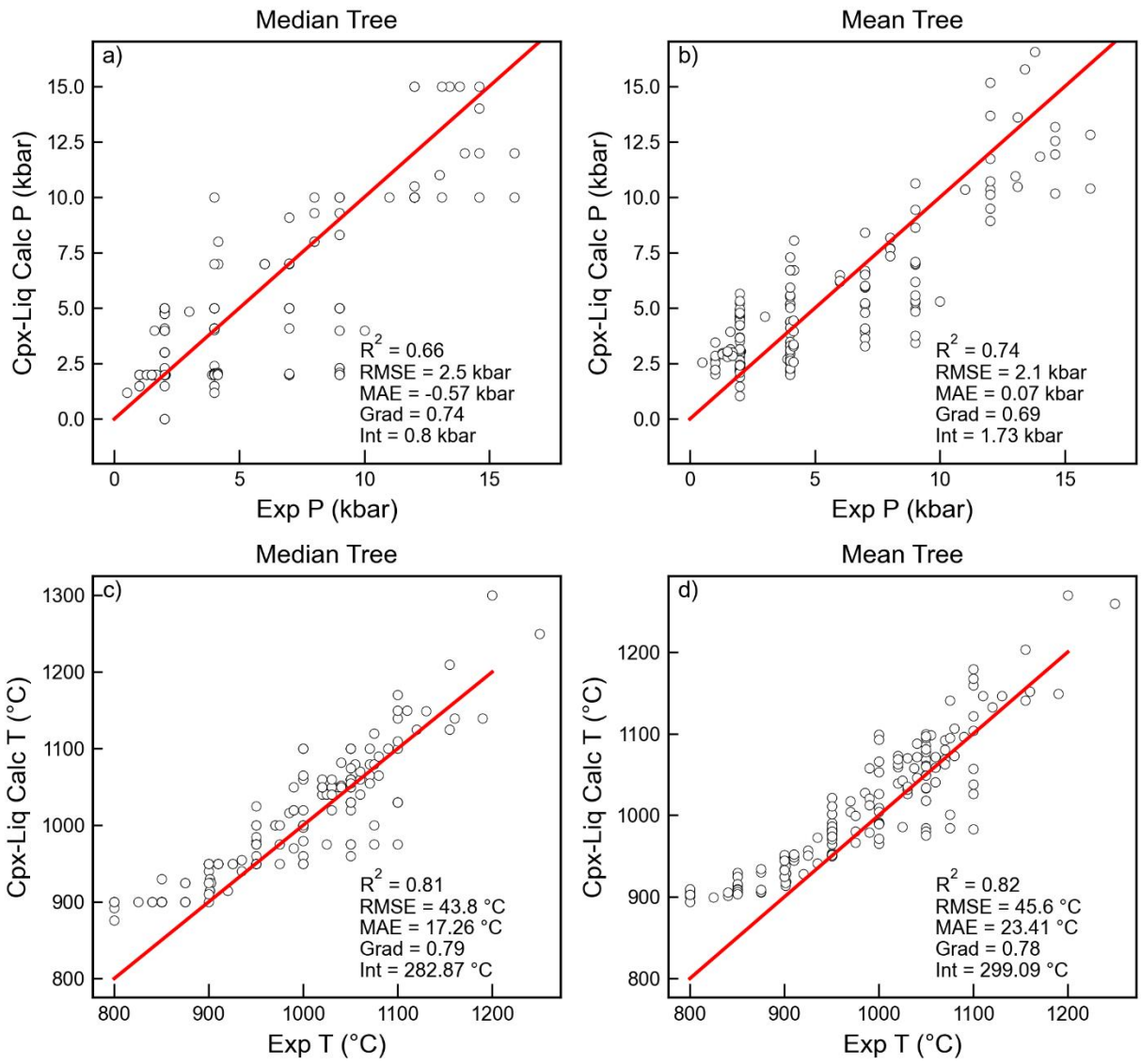

Supporting Fig 5 – Comparison of statistics using Median and mean tree for Cpx-Liq thermobarometry for Jorgenson et al. (2022).

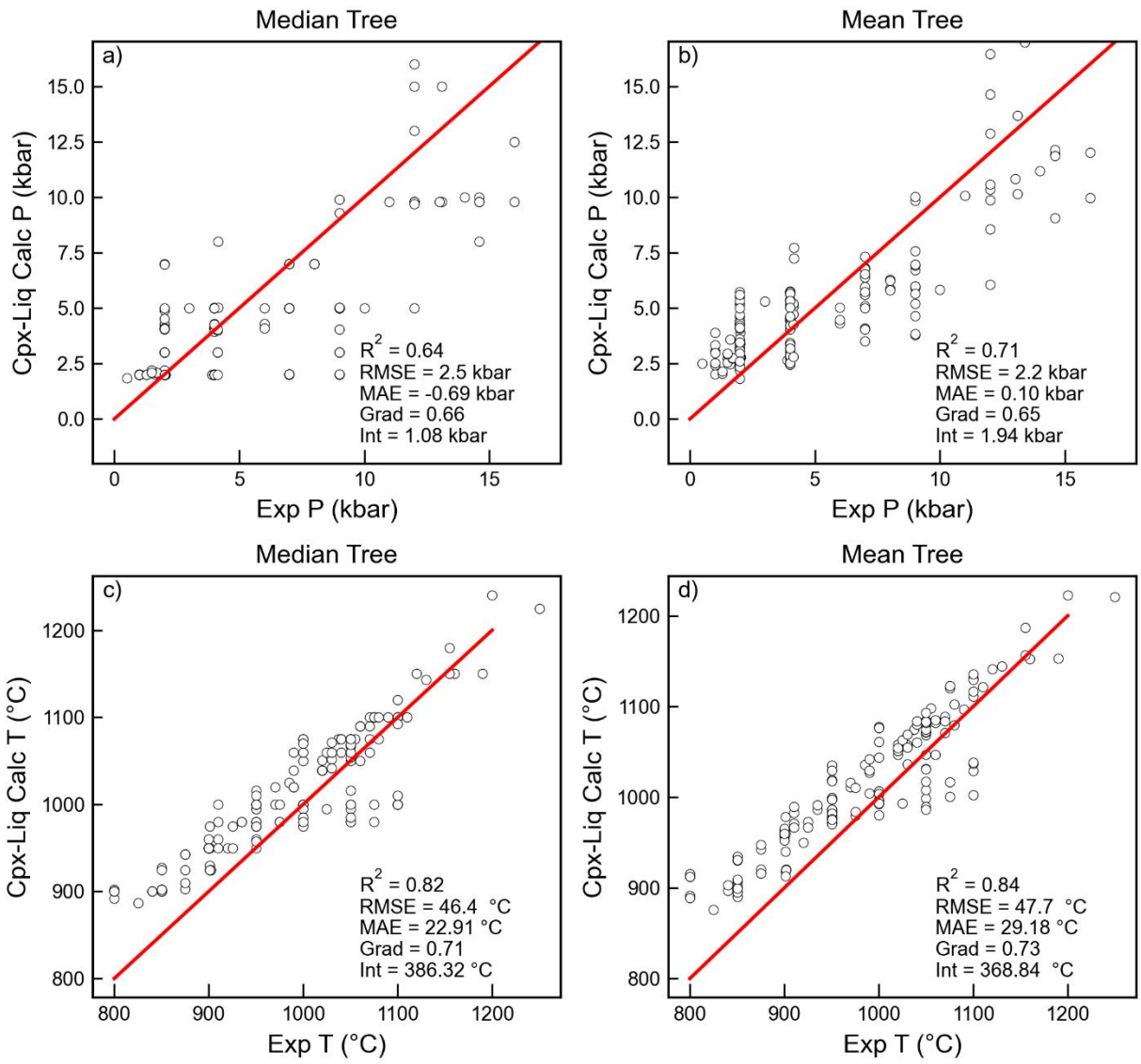

Supporting Fig. 6– Comparison of statistics using Median and mean tree for Cpx-Liq thermobarometry for Petrelli et al. (2020).

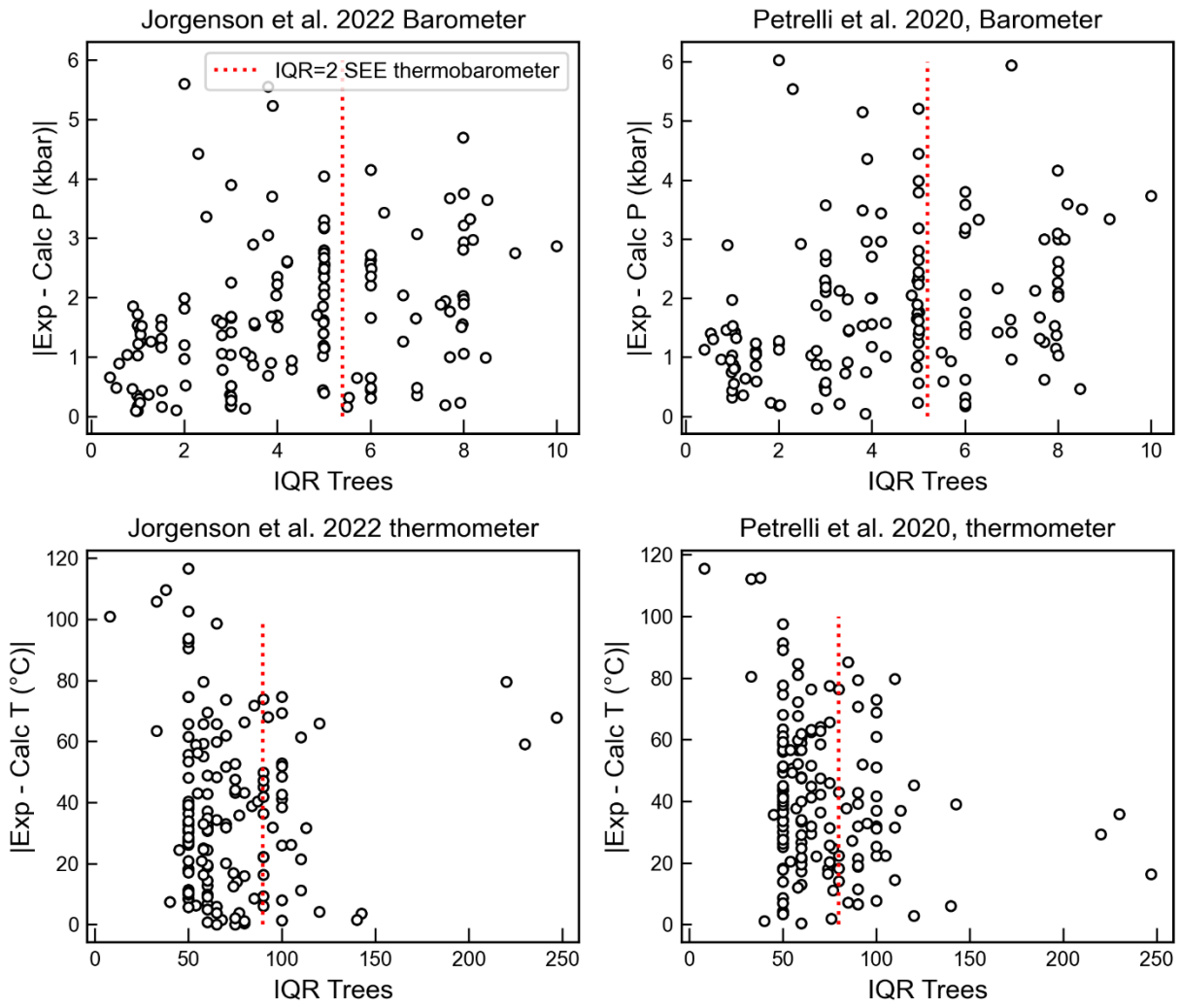

Supporting Fig. 7– Discrepancy of calculated Cpx-Liq P and T vs. the IQR of each regression tree. Jorgenson et al. suggest removing results with an IQR more than twice the stated SEE on the thermobarometer (e.g. to the right of the red dashed line). There is no clear correlation between the IQR and the absolute offset between calculated and experimental pressures and temperatures. We note that Petrelli don't release a Cpx-only barometer, we calibrate one using their dataset and the same regression tree mechanism used for P.

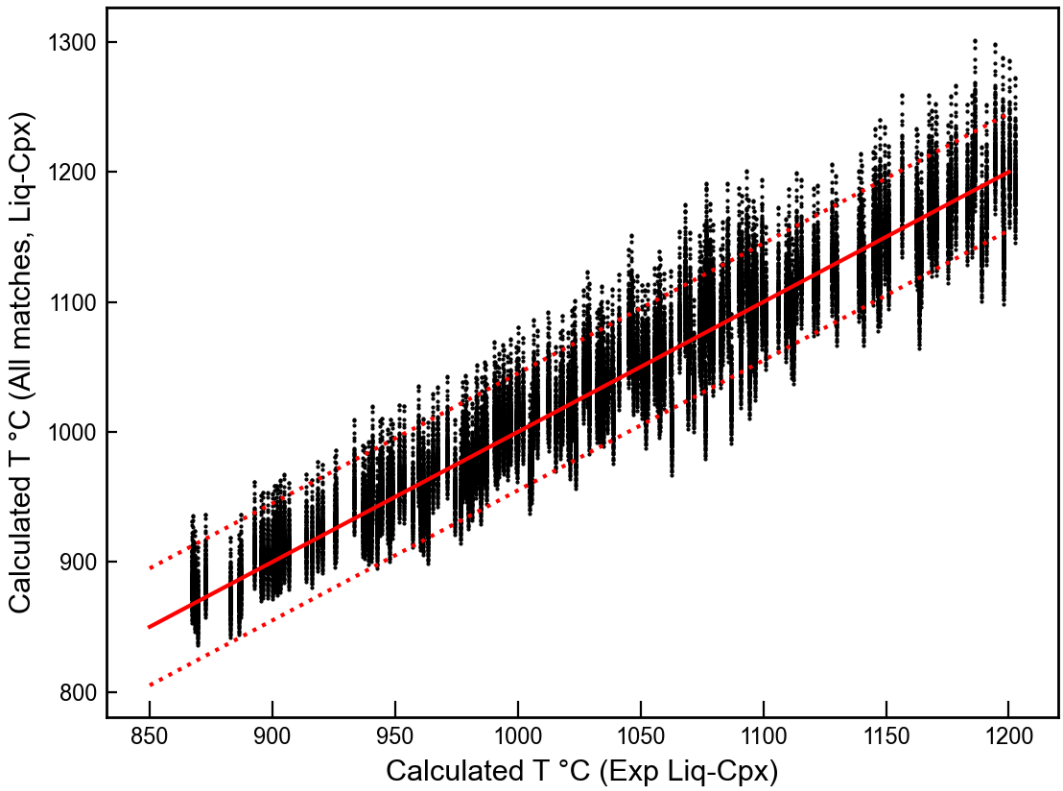

Supporting Fig 8 – Assessing the influence of the Cpx composition on the Cpx-Liq temperature. For each experimental Cpx-Liq pair we calculate the temperature using equation 33 of Putirka (2008), and plot this on the x axis. We then consider all possible Cpx-Liq matches, so each liquid gets matched to all N=194 Cpx compositions. We calculate the temperature for each of these pairs, resulting in N=194 dots sitting above each x axis coordinate. The y scatter is relatively small, the offset in calculated temperature for changing the Cpx composition is comparable to the quoted RMSE on the thermometer (shown by red dashed lines about the 1:1 red solid line). We use the average experimental pressure of the entire experimental database for all calculations.

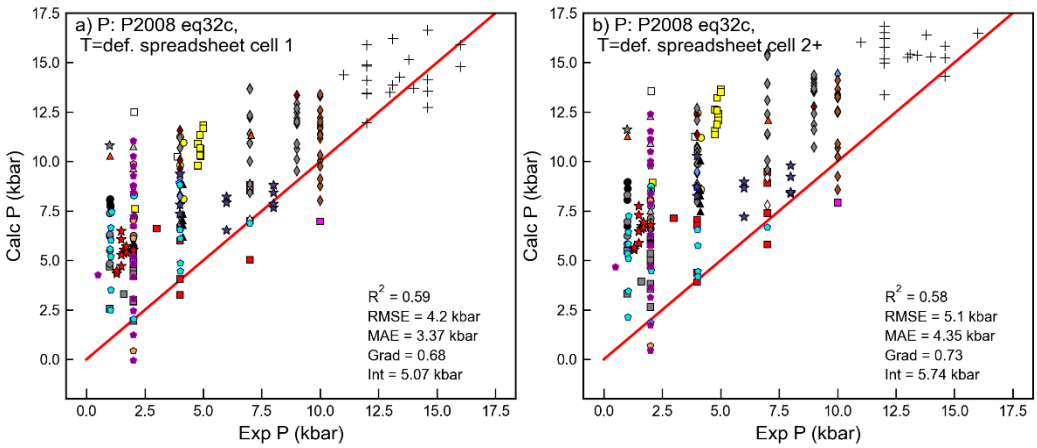

Supporting Fig. 9 – Comparing calculated and experimental pressures for the two ways Eq32c is used in the P2008 spreadsheets (the first cell vs later cells). We do not know for any given study how they dragged the cells down.

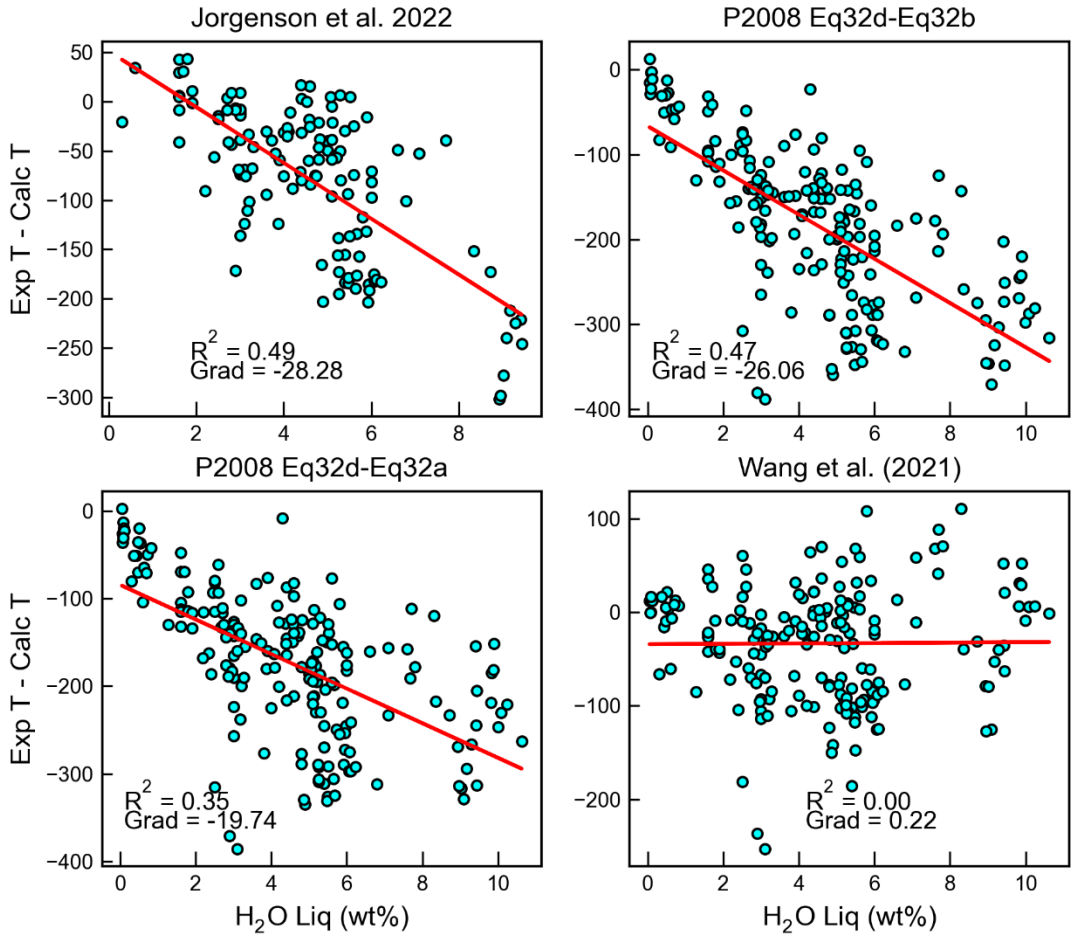

Supporting Fig 10 – Discrepancy between Cpx-only temperatures and melt water contents. Only the thermometer of Wang et al. (2021) has a term for H_2O content in the liquid.

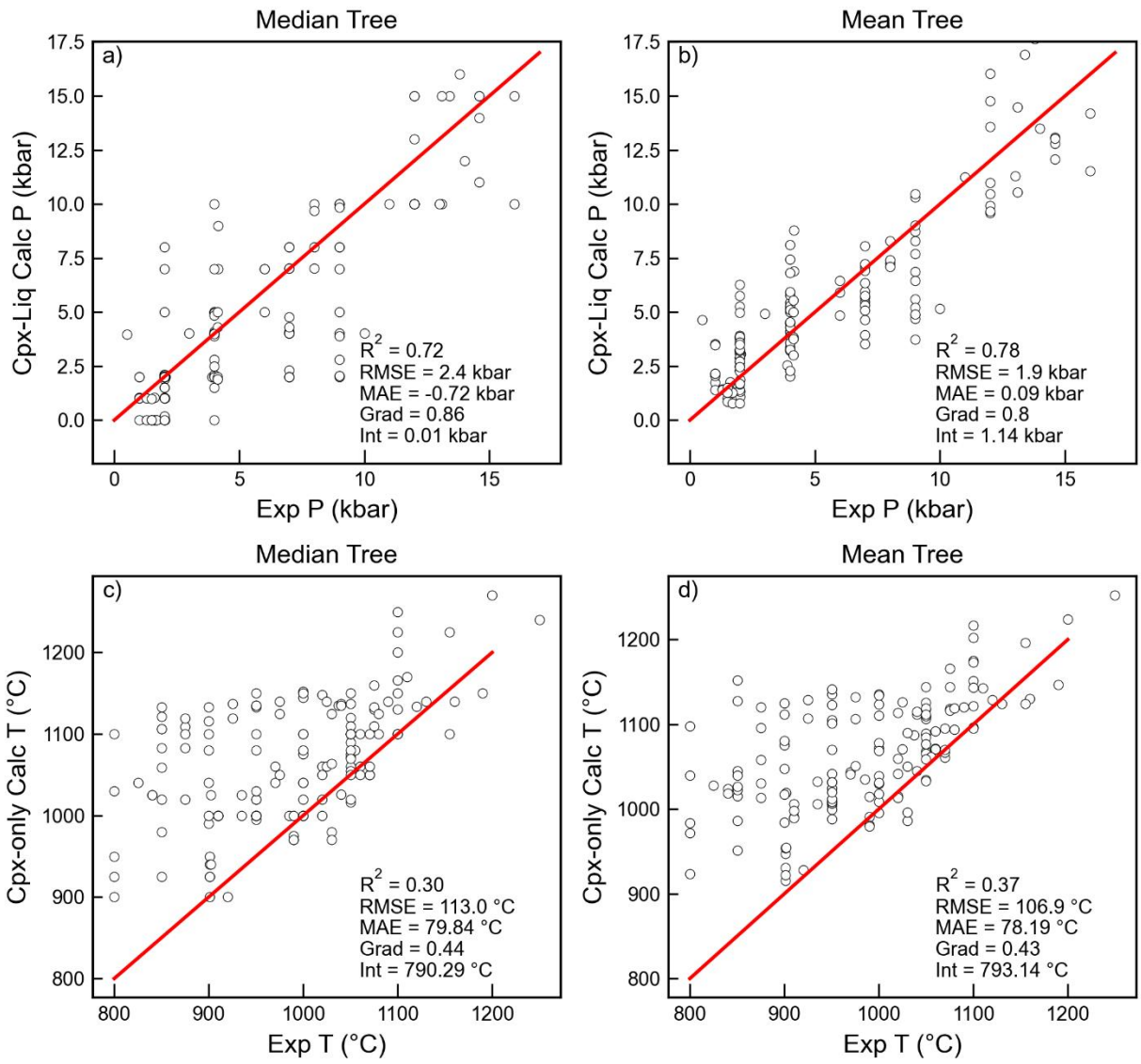

Supporting Fig 11 – Comparison of statistics using Median and mean tree for Cpx-only thermobarometry for Jorgenson et al. (2022).

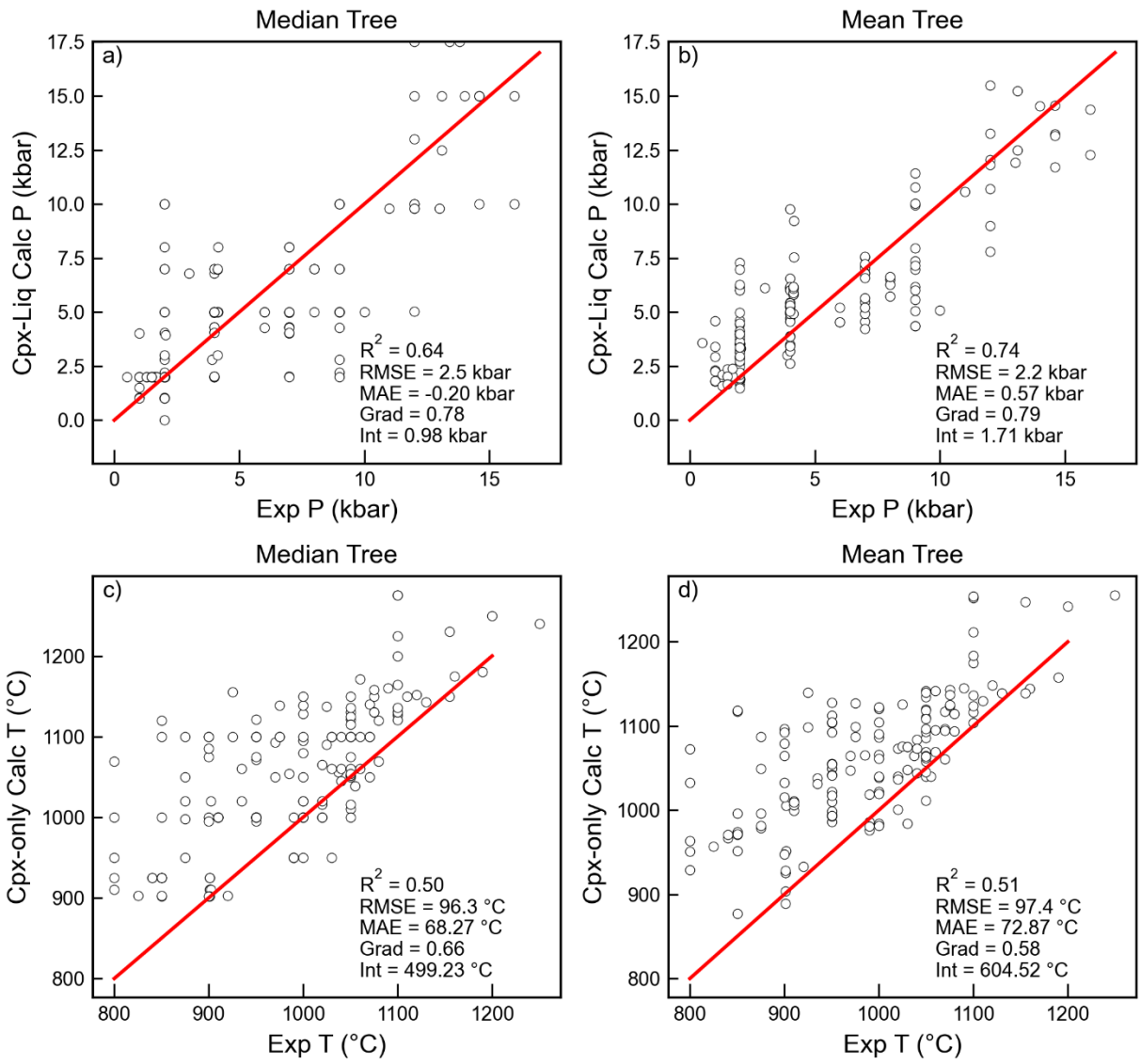

Supporting Fig. 12 – Comparison of statistics using Median and mean tree for Cpx-Liq and Cpx-only thermobarometry for Petrelli et al. (2020). No Cpx-only thermometer was officially published, we use the same regression strategy as for pressure to yield temperature.

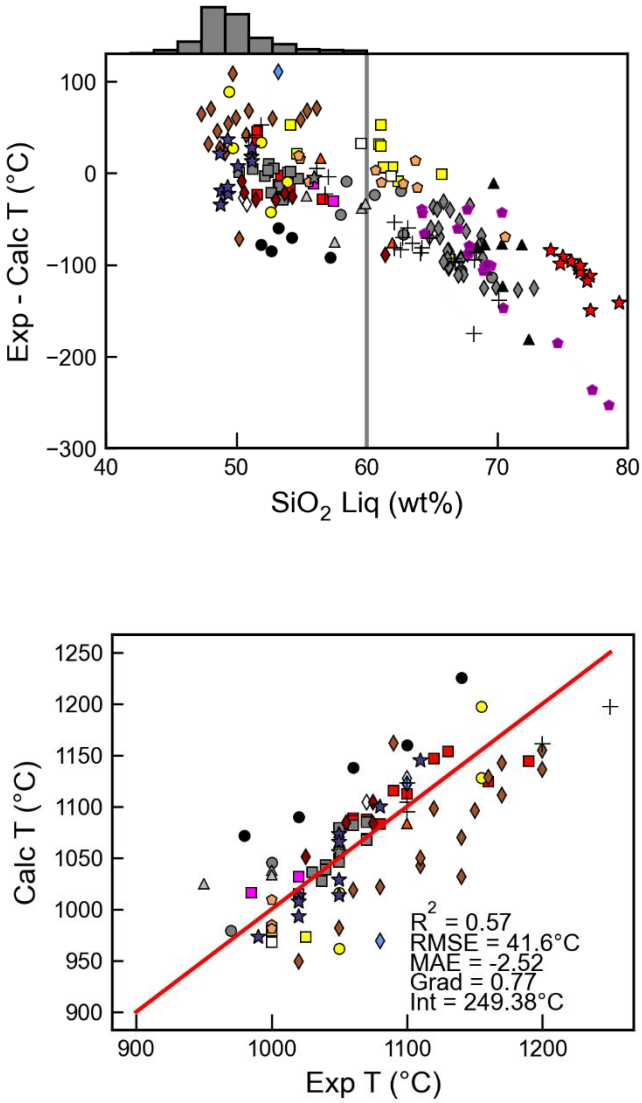

Supporting Fig 13 – Discrepancy between experimental and calculated Cpx-only temperatures using Wang et al. (2021) correlates strongly with SiO_2 when applied to Cpx grown from liquids which are more evolved than the calibration range of the model (shown by the grey histogram). Using only experiments with <60 wt% SiO2 results in a far better statistics than shown in the main text.

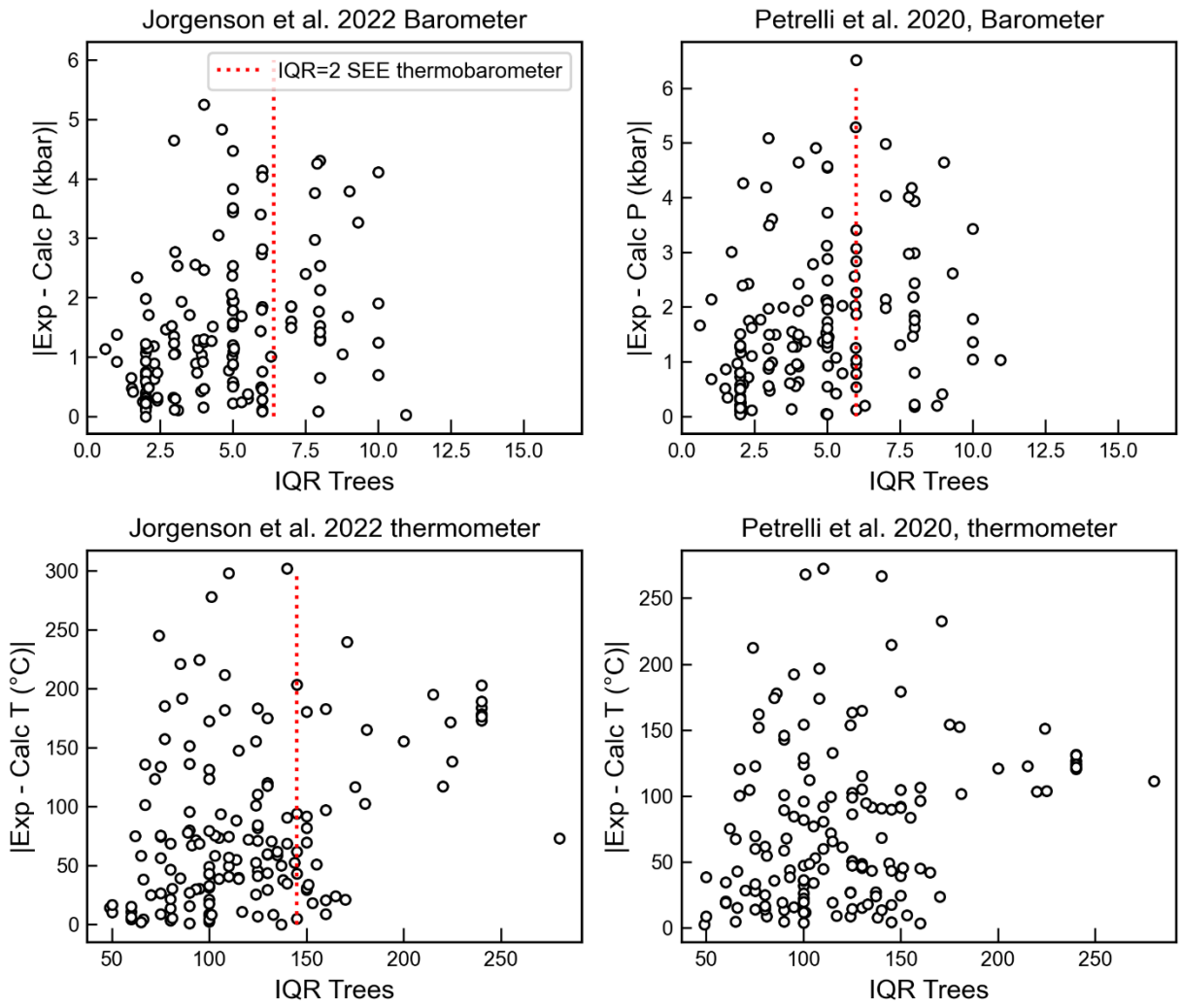

Supporting Fig. 14 – Discrepancy of calculated Cpx-only P and T vs. the IQR of each regression tree. Jorgenson et al. suggest removing results with an IQR more than twice the stated SEE on the thermobarometer (e.g. to the right of the red dashed line). There is no clear correlation between the IQR and the absolute offset between calculated and experimental pressures and temperatures. We note that Petrelli don't release a Cpx-only barometer, we calibrate one using their dataset and the same regression tree mechanism used for P.

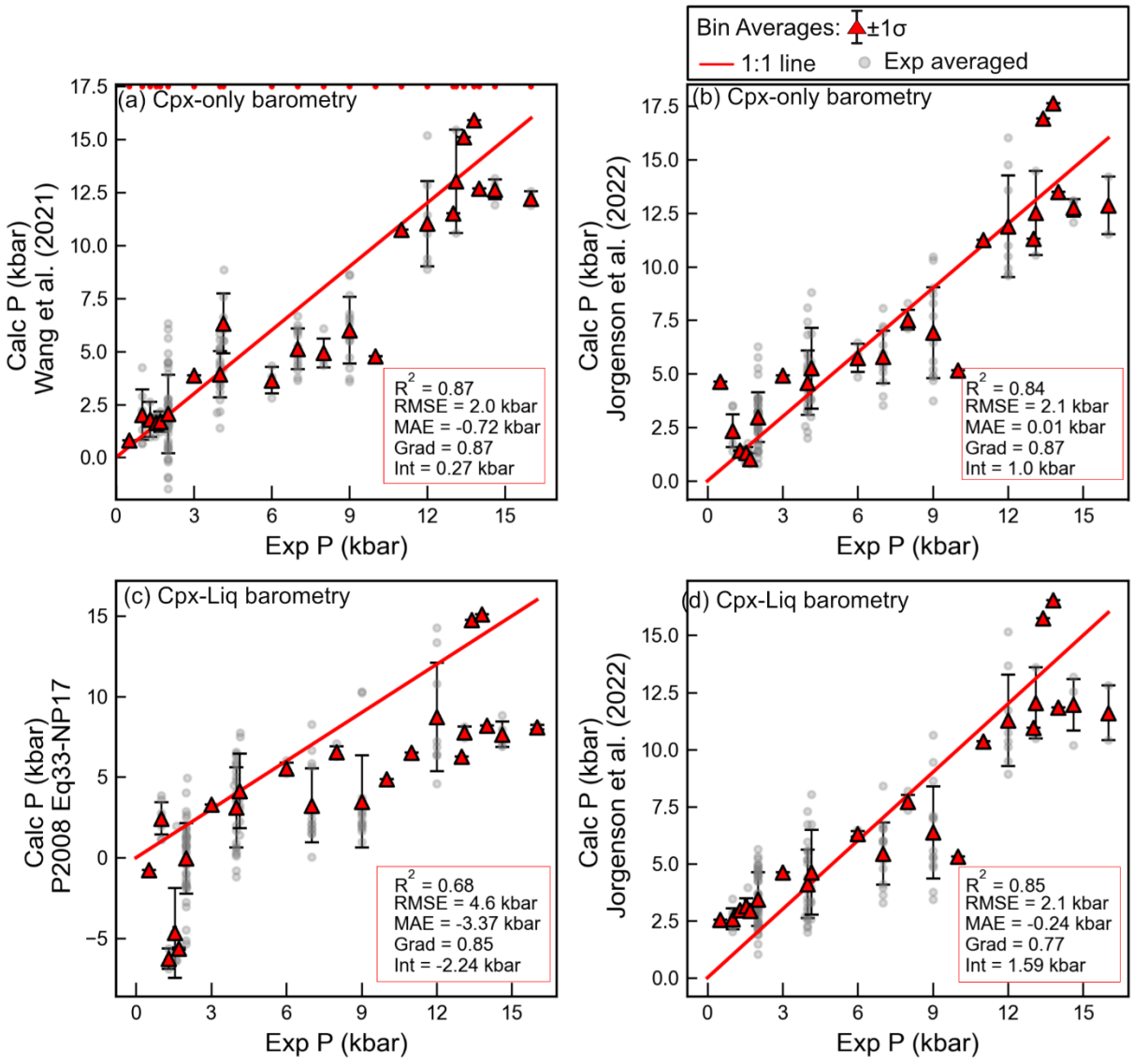

Supporting Fig. 15 – As for Fig 15 in the main text, but using bin averages even when there was only 1 experiment.